Longitudinal alterations in bone morphometry, mechanical integrity and composition in Type-2 diabetes in a Zucker diabetic fatty (ZDF) rat

Genna E Monahan, Jessica Schiavi-Tritz, Marissa Britton, Ted J Vaughan

Bone 170 (2023) 116672

Contents lists available at ScienceDirect

Bone

journal homepage: www.elsevier.com/locate/bone

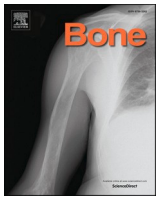

Full Length Article

Longitudinal alterations in bone morphometry, mechanical integrity and composition in Type-2 diabetes in a Zucker diabetic fatty (ZDF) rat

Genna E. Monahan [a], Jessica Schiavi-Tritz [a,b], Marissa Britton [a], Ted J. Vaughan [a,*]

[a] Biomechanics Research Centre (BioMEC), Biomedical Engineering, College of Science and Engineering, University of Galway, Galway, Ireland
[b] Laboratoire Réactions et Génie des Procédés, Université de Lorraine, CNRS UMR, 7274 Nancy, France

ARTICLE INFO

Keywords:
Type-2 diabetes
Bone biomechanics
Non-enzymatic glycation
Fourier transform-infrared micro-spectroscopy
Bone quality

ABSTRACT

Individuals with Type-2 Diabetes (T2D) have an increased risk of bone fracture, without a reduction in bone mineral density. It is hypothesised that the hyperglycaemic state caused by T2D forms an excess of Advanced Glycated End-products (AGEs) in the organic matrix of bone, which are thought to stiffen the collagen network and lead to impaired mechanical properties. However, the mechanisms are not well understood. This study aimed to investigate the geometrical, structural and material properties of diabetic cortical bone during the development and progression of T2D in ZDF (*fa/fa*) rats at 12-, 26- and 46-weeks of age. Longitudinal bone growth was impaired as early as 12-weeks of age and by 46-weeks bone size was significantly reduced in ZDF (*fa/fa*) rats *versus* controls (*fa/+*). Diabetic rats had significant structural deficits, such as bending rigidity, ultimate moment and energy-to-failure measured *via* three-point bend testing. Tissue material properties, measured by taking bone geometry into account, were altered as the disease progressed, with significant reductions in yield and ultimate strength for ZDF (*fa/fa*) rats at 46-weeks. FTIR analysis on cortical bone powder demonstrated that the tissue material deficits coincided with changes in tissue composition, in ZDF (*fa/fa*) rats with long-term diabetes having a reduced carbonate:phosphate ratio and increased acid phosphate content when compared to age-matched controls, indicative of an altered bone turnover process. AGE accumulation, measured *via* fluorescent assays, was higher in the skin of ZDF (*fa/fa*) rats with long-term T2D, bone AGEs did not differ between strains and neither AGEs correlated with bone strength. In conclusion, bone fragility in the diabetic ZDF (fa/fa) rats likely occurs through a multifactorial mechanism influenced initially by impaired bone growth and development and proceeding to an altered bone turnover process that reduces bone quality and impairs biomechanical properties as the disease progresses.

1. Introduction

Type-2 Diabetes (T2D) mellitus is a metabolic disorder that accounts for 90–95 % of overall diabetic cases [1]. Skeletal fragility is a major complication of T2D. Recently, it has been identified that T2D patients can have up to a 3-fold increased risk of bone fracture [2,3]. Moreover, disease duration may play a role, where individuals with long-term diabetes have a higher incidence of fracture than short-term diabetes [4,5]. Paradoxically, T2D is not accompanied by a reduction in bone mineral density (BMD), which is highly implicated in other bone diseases such as osteoporosis [6]. In fact, it has been found that patients with T2D can present with higher bone mass, compared to non-diabetic controls [7]. This implies that T2D is associated with reduced bone *quality*, with recent studies indicating that sub-tissue alterations to the organic constituents of the bone matrix contribute to impaired biomechanical behaviour [2,8–10]. During T2D, elevated levels of glucose, due to hyperglycaemia, results in an increased accumulation of non-enzymatic cross-links in the form of advanced glycated end-products (AGEs) [11,12], which are thought to stiffen the collagen leading to a more brittle behaviour. While it has been widely hypothesised that AGE cross-links are the primary cause of T2D bone fragility [2,13,15,16], there remains limited experimental evidence that provides a mechanistic link between AGE accumulation and tissue mechanics in T2D.

Much of the current understanding of the mechanics of bone fragility in T2D has been generated using *in-vitro* glycation models [17–21], whereby animal or human tissue was immersed in a ribose solution to facilitate non-enzymatic glycation of the protein network. In some cases, studies have found only subtle changes in mechanical properties [17,18]

* Corresponding author at: Biomechanics Research Centre (BMEC), Biomedical Engineering, University of Galway, Galway, Ireland.
E-mail address: ted.vaughan@nuigalway.ie (T.J. Vaughan).

https://doi.org/10.1016/j.bone.2023.116672
Received 4 November 2022; Received in revised form 30 December 2022; Accepted 3 January 2023
Available online 13 January 2023

despite significant increases in AGE accumulation. Other studies have found that AGE accumulation primarily affects the post-yield and toughness properties of the tissue [19,20]. In particular, Poundarik *et al* [21] investigated *in-vitro* glycated human cortical bone and found that fluorescent Advanced Glycation End-products (fAGE) accumulation was two-times greater and fracture toughness was reduced in the *in-vitro* glycated tissue *versus* the controls. However, these *in-vitro* glycation models are severely limited by the fact that they generate AGE levels in the tissue much higher than what occurs physiologically. Meanwhile, the difficulty in obtaining direct measurements *in-vivo* means that quantitative data describing precisely how bone tissue properties are impaired in patients with T2D is limited. To date, most human studies have focused on compression of trabecular cores [22,23], where it is difficult to decouple structural and material properties [22,23]. Notably, it has been found that cortical indentation distances from femoral neck bone has a negative correlation between serum total AGEs, but trabecular bone AGEs showed a positive correlation between compressive yield stress and strain [23]. Alternatively, animal studies can provide a wider understanding of the etiology of skeletal fragility in diabetes since confounding factors such as disease duration and gender can be controlled. There is currently no single animal model that can represent all features of Type-2 diabetes in humans. Hence, further animal studies are required to gain a wider understanding of each strain and get an idea as to which strains closely mimic type-2 diabetes in humans. Moreover, the advantage of the Zucker Diabetic Fatty (ZDF) *(fa/fa)* strain is that it is a well-established animal model of T2D, and the onset and progression of the disease is well understood [24–32]. Moreover, these rats develop T2D between 9 and 11 weeks of age before they have become skeletally mature (occurring at ~12-weeks). This animal model may provide a wider understanding of the progression of the disease in a population that develops T2D during puberty. Many studies of animals with diabetes have examined bone mechanical properties. Yet, there is a lack of animal research that has examined how AGE accumulation actually relates to bone fragility as the disease progresses.

Reinwald *et al.* investigated skeletal fragility of the femoral and L4 vertebral bone in ZDF *(fa/fa)* and Zucker Diabetic Sprague Dawley (ZDSD) rats at 33-weeks of age [33]. Both strains had a lower bone mineral content than controls, which coincided with the structural deficits found for femoral and vertebral bone after monotonic loading. Both strains had no difference in material properties for femoral bone in comparison to controls, however, ZDF (*fa/fa*) rats had a lower vertebral ultimate stress and modulus than controls. While the ZDSD rats showed similar results and had a lower bone toughness than controls, this study did not evaluate AGE content in tissue. The University of California, Davis (UCD)-T2DM rat has also been used, where it has been found that diabetic rats had a higher concentration of cortical bone AGEs than controls at 6 months of age [34]. Under monotonic loading, ulnar bone from diabetic rats had a significant reduction in bending rigidity, yield moment, elastic modulus, yield and ultimate stress. Conversely, Prisby *et al.* explored mechanical properties of ZDF femoral and tibial bone at 7 (short-term), 12- and 20- (long-term) weeks of age and found that, although structural deficits were observed in the long-term diabetic femora and tibia, there were no material-level differences observed [35]. While AGE content was again not measured in this study, other studies have investigated, in detail, changes in bone composition during T2D. Creecy *et al.* have used Raman spectroscopy and high performance liquid chromatography (HPLC) on ZDSD rat femoral bone to quantify cortical tissue composition at 16-, 22- and 29-weeks [36]. Raman spectroscopy results showed that ZDSD rats at 29-weeks had higher mineral:matrix ratio and crystallinity. HPLC results demonstrated no difference in levels of pentosidine (a non-enzymatic crosslink) between strains at any ages, although a significant increase with age was seen in the diabetic cohort. They found ultimate stress and fracture toughness of femurs at 16- and 22-weeks old ZDSD rats was higher than controls but showed no difference between strains at 29-weeks; ZDSD radius bone had reduced toughness at 29-weeks [36]. While alterations at the sub-tissue level of the bone matrix likely play a role in diabetic bone fragility, there are a lack of combined studies that investigate in detail how such sub-tissue properties are related to the mechanical properties of type-2 diabetic tissue [37–42]. Furthermore, longitudinal animal studies that consider older long-term diabetic time-points are required to understand how disease duration affects AGE accumulation and skeletal fragility.

This study conducts a longitudinal investigation on the geometrical, structural and material properties of T2D bone using a Zucker Diabetic Fatty (ZDF) (*fa/fa*) rat model over a 46-week period (~ one year old). Specifically, we hypothesize that cortical bone of the Zucker Diabetic Fatty (*fa/fa*) rats will have an impaired mechanical integrity, particularly as the duration of the disease increases which in turn will be accompanied by altered bone composition of the cortical tissue in comparison to the Zucker Lean (*fa/+*) control rats. The objectives of this study are to (i) examine geometrical alterations in type-2 diabetic and control cortical bones at various ages using micro-computed tomography; (ii) assess the fracture mechanics of cortical bone at the structural- and tissue-levels using a three-point bend test; (iii) explore the composition of diabetic cortical bone tissue and skin using FTIR and fluorescence AGE (fAGE) analysis; and (iv) investigate a correlation between cortical bone tissue composition and its fragility in T2D.

2. Materials and methods

2.1. Animal model and tissues

2.1.1. Animal model

A longitudinal 46-week study using male Zucker Diabetic Fatty [(ZDF: *fa/fa*) (T2D) and Zucker Lean (ZL: *fa/+*) (Control)] (Charles River, France) rats at 12-, 26- and 46-weeks of age (n = 7–9, per age, per condition) was conducted to investigate the geometrical, structural and material properties of bone in T2D at various metabolic stages throughout the life of the animal. Animals arrived at approximately 8- to 10-weeks old and were maintained under standard environmental conditions, with temperature maintained at 20–24 °C, humidity maintained at 45–50 %, and a 12 h light/dark cycle with food and water *ad libitum*. At 10-weeks old, ZDF and ZL rats were switched from a normal to a high fat diet (HFD) to induce a hyperglycaemic state in these rats, which causes overt diabetes (Formulab Diet 5008, LabDiet, St. Louis, USA (17 % kcal from Fat)). The animals were handled in accordance with the European Guidelines for Care and Use of Laboratory Animals (Directive 2010/63/EU). The Animal Care Research Ethics Committee (ACREC) in the National University of Ireland in Galway approved this project. In total, three rats died or were euthanized due to weight loss >10 % of their body weight or health issues. ZDF (*fa/fa*) rats which exhibited Lean rat characteristics were excluded from the dataset and *vice versa*. Supplemental Fig. S1 shows a timeline of the animal study over a 14-month period.

Rats were euthanized at 12- (Early-stage diabetes), 26- (Established diabetes) and 46-weeks (Long-term diabetes) of age. The blood glucose levels were recorded on the day of sacrifice with a glucometer to check the diabetic state of the animals. However, data recorded from the glucometer are not reported here as the glucometer could not accurately measure blood glucose values >33 mmol/L. After measuring their weight, right ulnae, radius bone and skin samples were dissected, wrapped in gauze wetted with PBS (ulnae, radius) or soaked in PBS (skin) then frozen at −20 °C. In this study, the ulna was used for biomechanical and compositional analysis as they had a slender and flat shape, reducing the effect of slipping during three-point bend testing. Moreover, it is understood that the most common fracture regions for T2D patients are the hip [43], vertebrae [44] and wrist [7]. Although femurs are commonly used in assessing fracture probability in the femoral and hip region, there are a lack of studies that explore fracture risk in bones associated with the wrist region in diabetes. The radius was used for fAGE analysis to measure AGE accumulation from cortical bone

in a region approximate to the ulna. Blood serum was collected on the day of euthanasia and frozen at −80 °C until analysis. Before experimentation, bones were removed from freezer into the fridge for defrosting for 12 h. Microarchitectural, biomechanical and compositional analysis was carried out to analyse local and systemic factors influenced by T2D. Right ulnae underwent X-Ray Micro-computed Tomography (micro-CT) scanning to determine geometric and morphometric properties, followed by a mechanical characterization through three-point bend testing, after which, a biochemical analysis was carried out. Cortical bone samples were sectioned from the mid-diaphysis and milled into a bone powder for FTIR analysis to measure various mineral- and collagen-properties, while skin and cortical bone sections were used to quantify AGE content through fAGE analysis (Fig. 1).

2.1.2. Serum analysis

Serum glucose levels were also measured to compare the hyperglycaemic state of the animals. Serum levels of insulin-like growth factor hormone I (IGF-I) were measured to explore the homeostasis of longitudinal bone growth and osteoblast function in type-2 diabetic rats. On the day of euthanasia, blood samples were collected by cardiac puncture from the rats and samples were left to clot at room temperature for 1–2 h. Blood samples were then centrifuged (Eppendorf 5424R microcentrifuge, Hamburg, Germany) at 2000 *g* for 15 min. Once the serum was separated from the clotted blood, the serum was aliquot into 1.5 mL Eppendorf tubes. Serum levels of glucose were measured using a quantitative glucose assay kit from Abcam (ab272532, Abcam, Cambridge, England) following the manufacturer's protocol. Briefly, the serum was diluted in sample dilution buffer provide with the kit by 4× and 2× for the ZDF (*fa/fa*) and ZL (*fa/+*), respectively. Samples and standards were added with 200 μL/well in duplicate to a 96-well plate. The absorbance was read at 630 nm. IGF-I was measured using an ELISA kit from AssayGenie (RTEB0037, AssayGenie, Dublin, Ireland) according to the manufacturer's protocol. Samples were diluted 1:100 and the microplate was read at 450 nm.

2.2. Geometric and morphometric properties

2.2.1. Bone size and shape

To compare the growth of lean (*fa/+*) and ZDF (*fa/fa*) rats, basic measurements of the ulna were taken using a Vernier Callipers before testing, which included bone length (L), anterior-posterior (AP) and medial-lateral (ML) diameters.

2.2.2. X-Ray Micro-Computed Tomography (μ-CT)

Right ulnae were imaged using a high-resolution micro-CT scanner (μCT100, Scanco Medical, Brüttisellen, Switzerland) at an isotropic voxel size of 5 μm. Scan settings used an X-Ray tube potential of 70 kVp, a current of 57 μA, an integration time of 500 ms at 1070 projections per 180° and a 0.5 mm thick aluminium filter was used to reduce beam-hardening artefacts. A 1.5 mm (300 slices, 62.4 min per bone) volume of interest (VOI) of cortical bone from the mid-diaphysis of the ulnae was scanned. Each slice was fitted with a contour around the periosteal and endosteal surface and segmented with a threshold of 710 mg HA/ cm^3 [45].

Using Scanco Image Processing Language, a series of structural and compositional parameters, which included polar moment of inertia (pMOI), medial-lateral and anterior-posterior moment of inertia (I_{ml} and I_{ap}), cross-sectional distance from the centroid to outermost point (C_{ml}), cortical area (Ct.Ar) cortical tissue material density (TMD), could be measured using previously published guidelines [46].

2.3. Structural and material properties

2.3.1. Quasi-static flexural testing

Following micro-CT imaging, mechanical testing of right ulnae samples was carried out until failure using a three-point bend test to measure whole-bone structural and material properties using a compression testing machine with a 2.5 kN load cell (Zwick/Roell, Ulm, Germany). Bones were kept hydrated at room temperature before testing. One sample was excluded from the 12-week old ZDF (*fa/fa*) group, as it was accidentally fractured during dissection. Load was applied to the medial aspect of the mid-diaphysis, with a pre-load of 0.4 N at a crosshead speed of 0.03 mm/s, over a support span of L = 7 x AP diameter. Force-displacement (F *vs.* d) curves were converted to moment-normalised displacement (*M vs. d'*) curves, according to Eqs. (1) and (2) and used to quantify bending rigidity (*k*) (slope of linear portion of curve), yield (found using 0.2 % offset method) and ultimate moment (maximum load experienced), post-yield displacement (PYD) (displacement that occurs between the yield and failure point) and energy-to-failure (area under the curve) (Fig. 2).

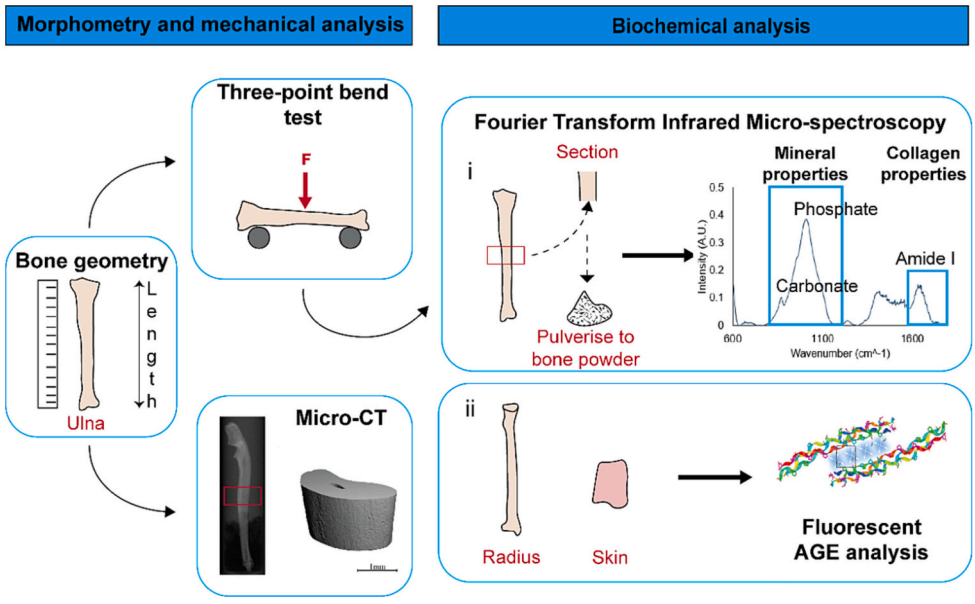

Fig. 1. Workflow of sample preparation methods and the tissue type used for each characterization technique; microarchitectural and biomechanical analysis using ulnae and compositional analysis, such as, (i) FTIR, (ii) fAGE analysis for demineralised cortical bone and skin sections.

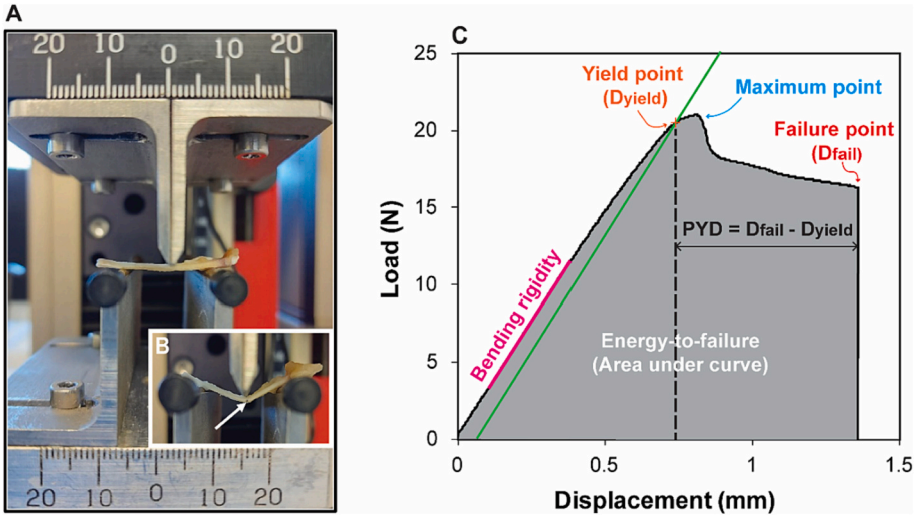

Fig. 2. (A) Initial set-up of the three-point bend test, (B) failure point reached and (C) a moment-normalised displacement curve from loading the right ulnae from rats until failure.

$$M = \frac{FL}{4} \tag{1}$$

$$d' = \frac{12d}{L^2} \tag{2}$$

Material properties (*e.g.*, Elastic modulus (E), Yield stress and strain, Ultimate stress (σ) and strain (ε) and toughness) were determined based on the equations below. Beam theory was used to convert M *vs* d' curves to stress-strain curves ((3)–(5)) [34,47]. Micro-CT derived images were used to quantify geometric parameters of I_{ml} and C_{ml}, based on the cross-sectional geometries obtained for each bone scan. These were determined using evaluation scripts in the Scanco Image Processing Language according to previously published guidelines [48]. In addition to reporting the estimated material properties using Eqs. (3)–(5), linear regression analysis was carried out to examine the intercept term and slope of ultimate moment *versus* section modulus (I_{ml}/C_{ml}) and compare variations between T2D (*fa/fa*) and control (*fa/+*) rats (see Supplementary Section C).

$$E = \frac{kL^3}{48I_{ml}} \tag{3}$$

$$\sigma = \frac{FLc_{ml}}{4I_{ml}} \tag{4}$$

$$(\varepsilon) = \frac{12c_{m_L}d}{L^2} \tag{5}$$

where, F = force; L = span length; *k* = bending rigidity; d = displacement.

2.4. Biochemical analysis

2.4.1. Fourier transform-infrared spectroscopy (FTIR) analysis

Attenuated total reflectance (ATR)-FTIR analysis was used to assess bone quality by examining mineral and collagen properties, such as, (1) mineral:matrix ratio, (2) carbonate:phosphate ratio (CP), (3) mineral crystallinity, (4) acid phosphate content (AP) and (5) collagen maturity (CM). A Spectral analysis protocol was developed using OriginPro 8 (OriginLab, Northampton, MA, USA) software and measure properties. Approximately 60 mg of cortical bone sectioned from the ulnar mid-shaft was used for FTIR after biomechanical testing. Bone was cleaned of surrounding tissue, bone marrow was removed, and bones were sectioned using a low-speed saw (Buehler Inc., Lake Bluff, IL). Bone sections were placed inside a sterile cryotube, 700 μL of distilled water (dH_2O) was added and bone was pulverised using a disperser (T10 Basic ULTRA-TURREX, IKA, Sigma Aldrich).

The powder-water mixture in the tubes were centrifuged (Eppendorf 5424R microcentrifuge, Hamburg, Germany) at 5000 *g* for 15 min to separate the powder from water. The water was pipetted out of the tube and discarded. The powders were left to dry in the tubes overnight on a hot plate at 37 °C. ATR-FTIR spectra were obtained (Spectral region: 600 to 4000 cm^{-1}, Resolution: 4 cm-1, Number of scans: 20, Mode: absorbance) (FTIR-8300 spectrometer, Shimadzu) from bone powders and three separate measurements were taken to get an average spectra for each sample. Spectra were baseline corrected and the mineral parameters included the mineral:matrix ratio (area ratio of the phosphate ν1 to ν3 peak [916 to 1180 cm^{-1}] to amide I peak [1596 to 1712 cm^{-1}]) [49] and the CP ratio (area ratio of the carbonate ν2 peak [852 to 890 cm^{-1}] to the phosphate ν1 to ν3 peak [916 to 1180 cm^{-1}]) [50,51]. Phosphate hidden sub-bands were determined in a 900–1200 cm^{-1} wavenumber range using second derivative hidden peaks and Savitzky-Golay smoothing method [50,52]. The sub-bands were Gaussian curve fit to the phosphate distribution [53,54], where mineral crystallinity (Ratio of areas at the peak of ≈ 1020 and ≈ 1030 cm^{-1}) [55–57] and AP (Ratio of areas at the peak of ≈ 1096 and 1127 cm^{-1}) [53,56,58,59] could be measured.

Finally, collagen-parameters were quantified by using second derivative analysis to fit the amide I band with seven Gaussian peaks (≈ 1610, 1630, 1645, 1661, 1678, 1692 and 1702 cm^{-1}) [42]. The area under each sub-peak was recorded and CM (Ratio of areas 1660 and 1692 cm^{-1}) – a proposed measurement pyridinoline to divalent cross-links [42,60,61].

2.4.2. Fluorescence Advanced Glycated End-Products (fAGE) analysis

AGEs accumulate in the bone as well as in various connective tissues throughout the body [12,62]. Total fAGEs were measured from skin and radius cortical bone sections using a fluorometric assay to quantify the level of AGEs present. Skin and bone sections were demineralised in 45 % formic acid for 8–10 days. Activated Papain Enzyme Digestion Solution (APEDS) was made up on the day of digestion by adding papain enzyme from papaya latex at a final concentration of 7.76 units/mL (P3125, Sigma Aldrich, St. Louis, MO) to 40 mL of papain buffer extract (100 mM sodium Phosphate Buffer/ 500 mM Na_2EDTA, pH 6.5) and 63 mg L-cysteine hydrochloride (C7477, Sigma Aldrich, St. Louis, MO). Skin and cortical bone sections of similar weight were placed into 1.5 mL black O-ringed micro-centrifuge tubes and 1 mL of APEDS solution as

added to each tube and rotated overnight at 10 rpm in an oven at 60 °C. Once fully digested, vortexed and quickly spun using a table-top centrifuge. Samples (100 μL of sample per tube) were lyophilised, then hydrolysed by adding 100 μL of 38 % HCl and then incubated in the oven at 110 °C for 20 h in the black O-ring tubes. Samples were then centrifuged at > 5000 *g* for 5 min and then left to dry on a hot plate for 48 h at 50 °C under a fume hood. Once the HCl had fully evaporated, 200 μL of ultra-pure water was added and samples were centrifuged at 15,000 *g* for 10 min and only the supernatant was used for analysis. A quinine assay was carried out to quantify the level of AGEs. Quinine standards were made up (serially dilution, 0, 0.5, 1, 2, 3.5, 5, 10 μg/mL, Stock: 10 μg/mL quinine per 1 mL of 0.1 N H_2SO_4) and 50 μL of the standards and 80 μL of the samples were added in duplicate to a black flat-bottomed 96-well plate. The fluorescence was measured using a plate reader (Synergy HT BioTek, Germany) at 360/460 nm excitation/ emission. Fluorescence of the samples was normalised against quinine standards.

Collagen content was measured from a hydroxyproline absorbance assay. A 1 mg/mL hydroxyproline solution was made up by adding 40 mg trans-4-Hydroxy-L-proline (H54409, Sigma Aldrich, St. Louis, MO) to 40 mL ultra-pure H_2O and was later used to create the hydroxyproline stock solution to make up the standards. Hydroxyproline standards were made up (0, 0.1, 0.25, 0.5, 1, 2, 5, 10 μg/mL, Stock: 50 μg/mL hydroxyproline per 1 mL of papain buffer extract). Skin and bone samples were diluted 50× with dH_2O for each age group, 60 μL of the samples and standards was added to a clear 96-well plate and absorbance was measured (570 nm excitation/ emission). The absorbance of samples was normalised against serially diluted hydroxyproline standards. The collagen content was derived based on prior knowledge that collagen consists of 14 % hydroxyproline [63,64]. Total fAGEs are reported in units of ng quinine/ mg collagen.

2.5. Statistical analysis

Normality and homogeneity of variances for all geometrical, biomechanical and compositional data were analysed using a Shapiro-Wilk test and homogeneity of variance was analysed with Levene's test using R statistical software (version R-4.1.0). Where normality and variance were not a concern, two-way ANOVA tests were carried out to (1) compare differences between each strain, followed by a multiple comparisons Bonferroni test and (2) compare differences within each strain across the different ages (12-, 26- and 46-weeks), followed by a multiple comparisons Tukey test (GraphPad Software, Inc., La Jolla, CA). If normality and variance was a concern, a Kruskal-Wallis test was used followed by the non-parametric Dunn's test to provide the adjusted *p*-value. Alpha levels of $p \leq 0.05$ were considered significant for a 95 % confidence interval. Data was pooled for all strains and ages when measuring correlation coefficients. The coefficients of correlation were calculated by Pearson's method. Data are represented as mean ± standard deviation.

3. Results

To assess the health of the animal, body mass and blood glucose levels were measured on the day of the euthanasia. In addition, IGF-I, one of the major growth factors involved in bone formation and development, was quantified in the serum in order to understand the differentiating function of the osteoblasts in T2D bone. Body mass was higher in T2D (*fa/fa*) rats compared to age-matched controls at 12- and 26-weeks of age (Table 1). However, some diabetic (*fa/fa*) rats showed signs of poor-health as the disease progressed. This was highlighted in various ways, through a decrease in movement, development of cataracts and a decreased food intake resulting in a loss of body mass. Long-term diabetic (*fa/fa*) rats (46-weeks) as a result had a 11.4 % ± 2.8 % ($p = 0.001$) reduction in body mass compared to 26-week diabetic rats and were, on average, 62.9 g (95 % CI: 29.28, 96.47, $p < 0.001$) lighter than age-matched controls (Supplementary Fig. S2).

Serum glucose levels were higher in diabetic (*fa/fa*) rats at all ages in comparison to controls (Table 1). Like the reduction in body mass of diabetic (*fa/fa*) rats from 26- to 46-weeks, serum glucose levels decreased, on average, by 38.8 % ($p < 0.001$) in long-term compared to established diabetic (*fa/fa*) rats as evidenced by a loss of appetite. Insulin growth factor hormone-I (IGF-I) levels of controls naturally declined by 38.7 % ($p = 0.03$) with age (12- to 46-weeks) in lean rats until there was no significant difference between T2D (*fa/fa*) and control (*fa/+*) IGF-I levels at 46-weeks. However, this natural decline with age did not occur in T2D (*fa/fa*) rats. In fact, diabetic (*fa/fa*) rats IGF-I levels tended ($p = 0.06$) to be lower than controls at 12-weeks of age and these levels did not change throughout any stage of diabetes in this ZDF (*fa/fa*) strain. There was a trending interaction between age and strain on IGF-I

Table 1
Animal body mass, serum, bone geometry and composition from μCT data.

	Control (*fa/+*)			T2D (*fa/fa*)		
	12 weeks[a] (n = 8–9)	26 weeks[b] (n = 8)	46 weeks (n = 7–9)	12 weeks[a] (n = 8–9)	26 weeks[b] (n = 8)	46 weeks (n = 7–9)
Body mass, g	293 ± 12.5	421 ± 27.9	466 ± 31.6	368 ± 19.4***	455 ± 32.2*	403 ± 33.1***
Serum glucose, mmol/L	12 ± 4.1	18 ± 4.9	12 ± 2.2	33.2 ± 6.9***	31 ± 5.9***	19 ± 2.6*, a, b
IGF-I, ng/mL	168 ± 72.7	155 ± 26.3	103 ± 31.9	105 ± 56.8^{+}	76 ± 28.4**	81 ± 31.5
Geometry						
Length, mm	31 ± 0.9	32 ± 1.1[a]	34 ± 0.8[a]	29 ± 1.1**	30.3 ± 0.9***	31 ± 1.0***, a
ML Diameter, mm	1.17 ± 0.02	1.20 ± 0.09	1.42 ± 0.1[a, b]	1.07 ± 0.02*	1.09 ± 0.06*	1.13 ± 0.08***
AP Diameter, mm	2.63 ± 0.2	2.65 ± 0.2	2.82 ± 0.2[a]	2.45 ± 0.05*	2.48 ± 0.13*	2.62 ± 0.13*, a
Aspect ratio	15.80 ± 1	15.57 ± 0.98	14 ± 1.13[a, b]	15.96 ± 0.49	15.89 ± 0.69	16.25 ± 1.14***
pMOI, mm^4	1.06 ± 0.21	1.71 ± 0.3[a]	2.16 ± 0.3[a, b]	0.82 ± 0.1*	1.16 ± 0.14***, a	1.255 ± 0.1***, a
I_{ml}, mm^4	0.14 ± 0.02	0.26 ± 0.03[a]	0.33 ± 0.04[a, b]	0.10 ± 0.01**	0.15 ± 0.01***, a	0.16 ± 0.01***, a
Ct.Ar, mm^2	1.99 ± 0.16	2.58 ± 0.13[a]	2.91 ± 0.16[a, b]	1.72 ± 0.08***	2.06 ± 0.1***, a	2.11 ± 0.07***, a
Composition (μCT)						
Ct.TMD, $mgHA/cm^3$	1155.9 ± 22.3	1250.5 ± 19.3[a]	1289 ± 4.1[a, b]	1134 ± 18.8*	1246.5 ± 16.4[a]	1285.3 ± 15.1[a, b]

Values are mean ± SD. T2D, Type-2 diabetic; IGF-I, Insulin growth factor hormone I; ML, Medial-lateral, AP, Anterior-posterior; pMOI, Polar moment of inertia; Iml, Medial-lateral moment of inertia; Ct.Ar, Cortical area, Ct.TMD, Cortical Tissue mineral density. Difference from aged matched lean control (*fa/+*) rats with * ($p < 0.05$), ** ($p < 0.01$), *** ($p < 0.001$) and $^{+}$ ($p = 0.06$) significance.

[a] Significantly different from 12-weeks determined by a multiple comparisons Tukey test.

[b] Significantly different from 26-weeks determined by a multiple comparisons Tukey test.

(Variation = 5.17 %, $p = 0.05$).

3.1. TMD between diabetic (*fa/fa*) and control (*fa/+*) rats did not change as the disease progressed

Since T2D is not often accompanied by a reduction in mineral density, the material tissue mineral density of cortical bone (Ct.TMD) was measured. Ct.TMD increased with age for control and ZDF (*fa/fa*) rats (Table 1). Ct.TMD of early stage (12-weeks) diabetic rats with 1134 ± 18.8 mg HA/cm^3 was lower than age-matched controls with 1155.9 ± 22.3 mg HA/cm^3 ($p = 0.04$). As the disease progressed, there was no difference in Ct.TMD between strains.

3.2. Cortical bone geometrical deficits related to rat strain

To further understand longitudinal bone growth and development during T2D, bone geometry was examined. Bone geometry was also required for beam theory analysis after mechanical testing. Ulnae in ZDF (*fa/fa*) rats were shorter in length and smaller in diameter compared to healthy controls at every stage of diabetes (Table 1). Similarly, geometrical properties, such as, polar moment of inertia (pMOI), medial-lateral moment of inertia (I_{ml}) and cortical bone area (Ct.Ar), measured from micro-CT data showed declines in bone size for diabetic (*fa/fa*) rats *versus* controls (*fa/+*) (Table 1). From 26- to 46-weeks of age, pMOI (+26.3 %), I_{ml} (+26.9 %) and Ct.Ar (+12.8 %) significantly ($p < 0.001$) increased for control rats. However, there was no difference in pMOI, I_{ml} and Ct.Ar of diabetic (*fa/fa*) rats, indicating that bone growth slowed between the established and long-term diabetic phase in this ZDF (*fa/fa*) strain.

3.3. Resistance to deformation and fracture and reduced ductility in diabetic (*fa/fa*) rat tissue

The structural properties of ulnar cortical bone were measured *via* three-point bend testing at all time-points (Fig. 3). The structural properties reflected the geometrical deficits of the diabetic (*fa/fa*) rat bones. Bending rigidity and ultimate moment significantly increased with age for control rats (Fig. 3 (A) & (B)). From 26- to 46-weeks in controls, bending rigidity and ultimate moment had increased by 23.3 % ($p < 0.01$) and 21.4 % ($p < 0.001$), respectively. The ability for cortical ulnar bone to resist deformation was 41.6 % ($p < 0.001$) and 52.6 % ($p < 0.001$) lower in established (26-weeks) and long-term (46-weeks) diabeteic (*fa/fa*) rats when compared to their age-matched controls, respectively.

Ultimate moment and whole bone strength of ZDF (*fa/fa*) rats were also significantly lower than age-matched controls at 12- (−20.4 %), 26- (−31.8 %) and 46-weeks (−43.8 %) old (Fig. 3 (B)). Energy-to-failure increased 1.5-fold ($p = 0.007$) in control rats from 12- to 46-weeks, while diabetic rats showed no increase in energy-to-failure with age. Conversely, from 26- to 46-weeks, energy-to-failure tended towards a decrease (Fig. 3 (C)) and long-term diabetic (*fa/fa*) rats had a significantly reduced ability to resist fracture in comparison to controls ($p < 0.01$). Rats with earlier stages of diabetes had a more ductile behaviour compared to controls at 12- ($p < 0.01$) and 26-weeks ($p < 0.05$) (Fig. 3 (D)). Yet, as these rats aged and the disease progressed, post-yield displacement reduced and was no longer greater than control bones,

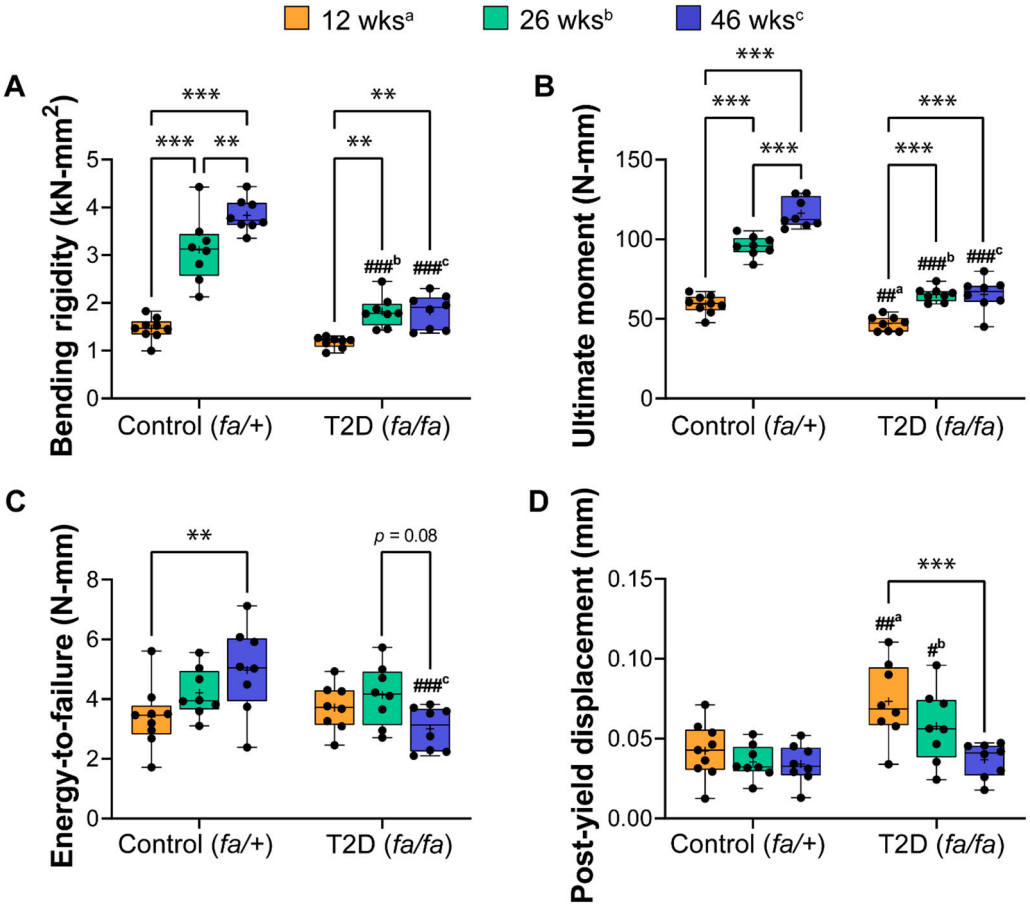

Fig. 3. Structural properties (A) bending rigidity, (B) ultimate moment, (C) energy-to-failure and (D) post-yield displacement measured from loading cortical ulnar rat bone until failure in a three-point bend configuration. * ($p < 0.05$), ** ($p < 0.01$) and *** ($p < 0.001$) significance within strain, # ($p < 0.05$), ## ($p < 0.01$) and ### ($p < 0.001$) significance between strain at 12 [a], 26 [b], and 46 [c] weeks.

indicating that bone ductility significantly reduced with long-term diabetes (Fig. 3 (D)).

3.4. Tissue material strength of diabetic (*fa/fa*) rats impaired as the disease progressed

Fig. 4 shows the tissue-level material properties, where bone geometry was considered to explore the tissue itself. Although the mean elastic modulus of diabetic (*fa/fa*) rats reduced by 7 % from 26- to 46-weeks, this was not significant ($p = 0.52$) (Fig. 4 (A)). Although disease duration did not affect tissue level modulus, it was found that tissue material strength was affected. Yield and ultimate stress increased with age from 12- to 46-weeks for control rats by 24.7 % and 20.6 % ($p < 0.001$), respectively (Fig. 4 (B) & (D)).

Furthermore, when examining strain-related differences, tissue yield and ultimate strength of rats with earlier stages of diabetes at 12- and 26-weeks were not different to those of the age-matched controls. Despite this, by 46-weeks of age, long-term diabetic (*fa/fa*) rats had a significantly lower tissue yield (−11.4 %) and ultimate (−11.3 %) ($p < 0.05$) strength in comparison to their age-matched controls (Fig. 4 (B) & (D)). This indicates that, at a material level, the tissue itself was impaired as the disease progressed, ultimately leading to a reduced bone strength. The toughness represents the area under the stress-strain curve and no differences were found between strains at each age. It was demonstrated that diabetic rats showed a trend towards a decrease in toughness from 12- to 46-weeks of age (−25.5 %) ($p = 0.08$), while there was no difference in toughness with age for controls. Additionally, a significant statistical interaction between strain and age on bone toughness was found (15.75 % of total variation, $p = 0.02$). A linear regression analysis was used to further explore the material strength by analysing ultimate modulus *versus* section modulus between strains at each age (see Supplementary Fig. S5). It was found that ultimate moment varied between strains at the various ages when section modulus is considered at 26- and 46-weeks. Control (*fa/+*) rats had a significantly higher material strength at 26- ($p < 0.05$) and 46-weeks ($p < 0.001$) in comparison to diabetic (*fa/fa*) rats.

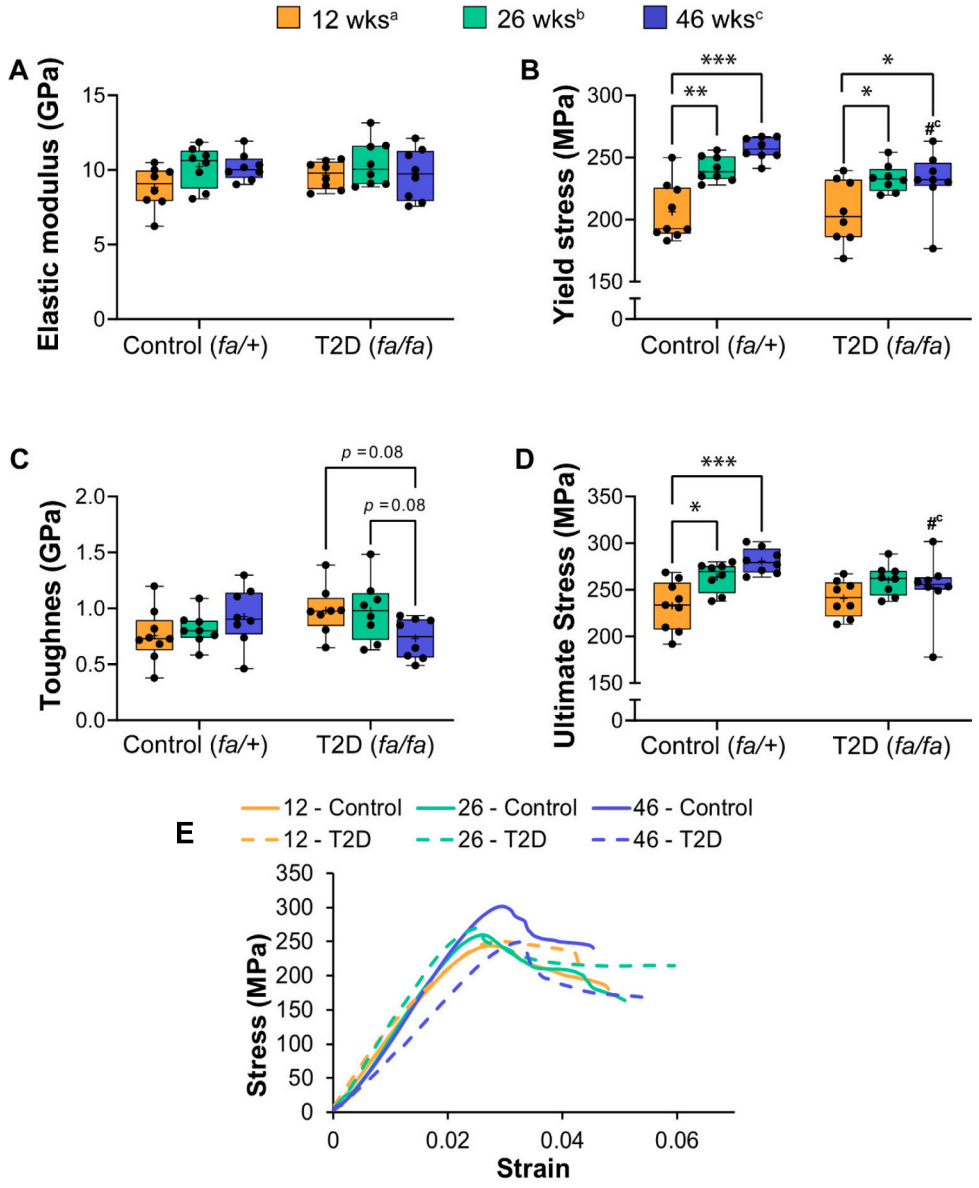

Fig. 4. Material properties: (A) elastic modulus, (B) yield stress, (C) toughness and (D) ultimate stress measured from a three-point bend test considering bone geometry. (E) Sample stress-strain curves per group. * ($p < 0.05$), ** ($p < 0.01$) and *** ($p < 0.001$) significance within rat strains, # ($p < 0.05$), ## ($p < 0.01$) and ### ($p < 0.001$) significance between rat strains at 12 [a], 26 [b], and 46 [c] weeks.

3.5. Individual mineral constituents altered in long-term diabetic (*fa/fa*) rat bone

FTIR was used to assess bone quality by examining various mineral- and collagen-properties. Carbonate:phosphate ratio (C:P ratio) increased from 12- to 46-weeks of age for ZDF (*fa/fa*) rats (+12.5 %, $p < 0.05$) and control (+25 %, $p < 0.001$) rats (Fig. 5 (B)). As the disease progressed, long-term diabetic rats had a 10 % reduction in C:P ratio in comparison to age-matched controls ($p < 0.05$). Acid phosphate content (AP content) reduced significantly from 12- to 26-weeks of age (−34 %, $p < 0.05$) but there was no difference in AP content from 26- to 46-weeks. On average, ZDF (*fa/fa*) rats had 13 % (95 % CI: 4 %, 21 %, $p < 0.01$) and 10 % (95 % CI: 1 %, 19 %, $p < 0.05$) more AP content than controls at 12- and 46-weeks of age, respectively (Fig. 5 (D)). There was no significant difference in mineral:matrix ratio, mineral crystallinity and collagen maturity (CM) between control (*fa/+*) and diabetic (*fa/fa*) rats at all ages (Table 2). However, collagen maturity exhibited a significant interaction on strain (Variation = 20.75 %, $p = 0.002$).

3.6. AGE accumulation increased in skin of long-term diabetic (*fa/fa*) rats but not bone

AGEs were measured from two tissue types: bone, to directly compare AGE-levels to the tissues' mechanical integrity and skin, to explore a surrogate marker of AGEs. Fig. 5 shows diabetic (*fa/fa*) rats at 46-weeks of age had 2-fold ($p < 0.001$) more AGEs present in the skin than controls (Fig. 5 (A)). There was no difference in the concentration of AGEs in the cortical bone between diabetic (*fa/fa*) and control (*fa/+*) rats at any age (Fig. 5 (C)). Skin AGEs exhibited a significant interaction between strain and age (Variation = 10.51 %, $p = 0.02$). Whereas bone AGEs only showed a trending interaction on age (Variation = 11 %, $p = 0.07$).

3.7. Correlation results among serum levels, skin and bone composition

All correlation results described in this section are shown in Supplementary Table S1. Mineral-properties measured *via* FTIR such as, C:P ratio and AP content were associated with serum glucose levels ($r = -0.33$, $p < 0.05$ and $r = 0.37$, $p < 0.05$, respectively). However, serum glucose levels and TMD showed no correlation. Fluorescent AGEs measured from skin and bone samples did not have a significant correlation with blood glucose levels. Interestingly, TMD and AP content were negatively correlated ($r = -0.46$, $p < 0.01$) (Supplementary Table S1). TMD was also positively correlated with the mineral-property, C:P ratio ($r = 0.35$, $p < 0.01$) (Supplementary Table S1). AGEs from bone tissue correlated positively with TMD (Bone $r = 0.33$, $p = 0.025$), yet skin AGEs did not (Supplementary Table S1).

3.8. Correlation results for biomechanical properties

Correlation results shown in this section were carried out to investigate if there was an association between AGEs and bone composition with the tissues mechanical integrity. Collagen maturity was positively associated with AGEs in the skin ($r = 0.33$, $p = 0.029$), but had no correlation with AGEs in bone (Supplementary Table S1). Yield and ultimate stress were not associated with AGEs in skin (Yield stress: $r = -0.13$, $p = 0.37$; Ultimate stress: $r = -0.14$, $p = 0.34$), or bone (Yield stress: $r = 0.021$, $p = 0.89$; Ultimate stress: $r = 0.017$, $p = 0.92$) (Fig. 6 (C) & (G)). Yield and ultimate stress were positively correlated with TMD (Fig. 6 (A) & (E)) ($r = 0.57$, $p < 0.001$ and $r = 0.45$, $p < 0.01$). However, it is clear that age has an influence on this correlation where at 12-weeks lower TMD levels correlate with lower yield and ultimate stresses and as rat's age and bones get bigger, TMD levels have increased and correlate to higher yield and ultimate stresses. Interestingly, Yield stress was negatively correlated with acid phosphate content ($r = -0.3$, $p < 0.05$) Fig. 6 (B)). Ultimate stress was positively associated with, the carbonate:phosphate ratio ($r = 0.33$, $p < 0.05$) (Fig. 6 (F)). Both carbonate:phosphate ratio and acid phosphate content were properties associated with the mineral component of the bone tissue. Bones extracellular matrix is made up of an organic (collagenous and non-collagenous proteins) and inorganic (hydroxyapatite and other minerals) component which affects bones toughness and strength,

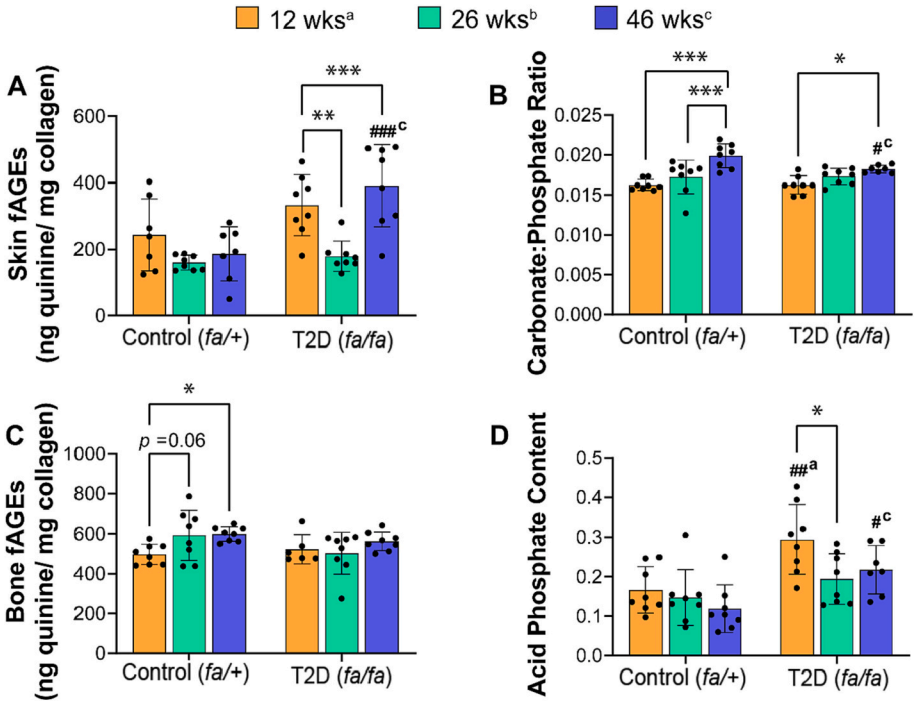

Fig. 5. Various compositional results from (A, C) fAGE analysis of cortical bone and skin sections from rats and (B, D) FTIR analysis of cortical ulnar bone measuring carbonate:phosphate ratio and acid phosphate content. * ($p < 0.05$), ** ($p < 0.01$) and *** ($p < 0.001$) significance within rat strains, # ($p < 0.05$), ## ($p < 0.01$) and ### ($p < 0.001$) significance between rat strains at 12 [a], 26 [b], and 46 [c] weeks.

Table 2
Compositional properties measured from ulnar cortical tissue obtained from rats as determined from Fourier transform-infrared spectroscopy (FTIR) analysis.

	Control (*fa/+*)			T2D (*fa/fa*)		
	12 weeks[a] (n = 8–9)	26 weeks[b] (n = 8)	46 weeks (n = 7–9)	12 weeks[a] (n = 8–9)	26 weeks[b] (n = 8)	46 weeks (n = 7–9)
Mineral:Matrix ratio	5.129 ± 0.94	4.83 ± 0.88	5.12 ± 0.86	5.68 ± 0.93	4.75 ± 0.86	5.40 ± 0.39
Carbonate:Phosphate ratio [++]	0.016 ± 0.0007	0.017 ± 0.002	0.020 ± 0.002[a, b]	0.016 ± 0.0011	0.017 ± 0.001	0.018 ± 0.0005*
Mineral Crystallinity	0.94 ± 0.23	1.07 ± 0.23	1.26 ± 0.57	1.00 ± 0.27	1.22 ± 0.31	1.02 ± 0.21
Acid Phosphate Content [+, ++]	0.17 ± 0.06	0.15 ± 0.07	0.12 ± 0.06	0.29 ± 0.09**	0.19 ± 0.06[a]	0.22 ± 0.06*
Collagen Maturity [+]	2.79 ± 0.41	3.14 ± 0.82	3.41 ± 0.83	3.75 ± 0.72	4.00 ± 1.19	4.09 ± 1.11

Values are mean ± SD. T2D, Type-2 diabetic; Difference from aged matched lean control (*fa/+*) rats with * ($p < 0.05$), ** ($p < 0.01$) and *** ($p < 0.001$) significance.
[a] Significantly different from 12-weeks determined by a multiple comparisons Tukey test.
[b] Significantly different from 26-weeks determined by a multiple comparisons Tukey test.
[+] Significant ANOVA interaction between strain.
[++] Significant ANOVA interaction between age.

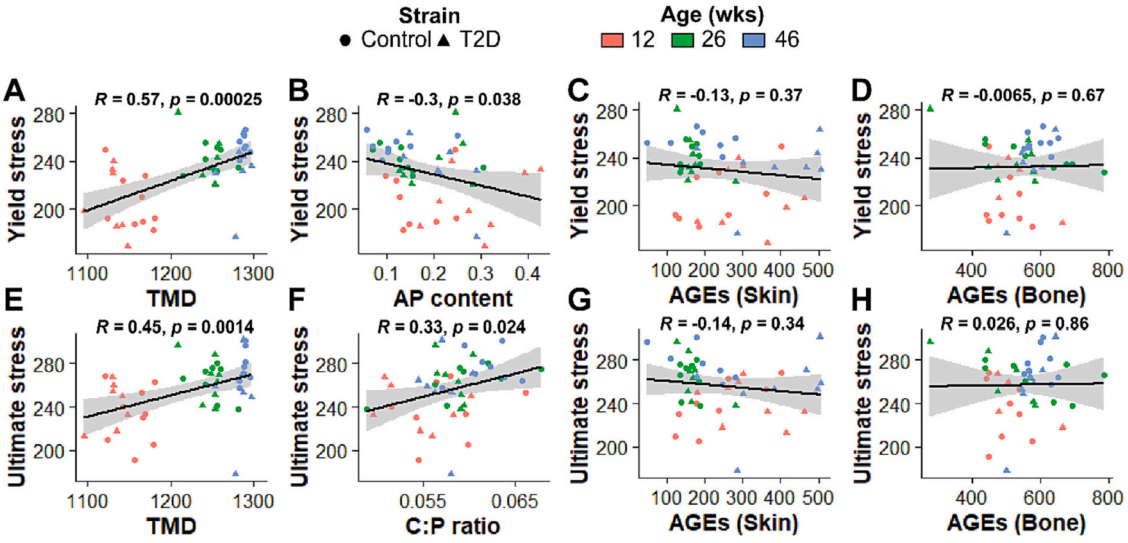

Fig. 6. Correlation results showing the association of the material properties yield stress with (A) tissue mineral density (TMD), (B) acid phosphate (AP) content, (C) AGEs in rat skin and (D) AGEs in rat bone; and ultimate stress with (E) tissue mineral density (TMD), (F) Carbonate:phosphate ratio (C:P), (G) AGEs in rat skin and (H) AGEs in rat bone.

respectively [65,66]. This further explains the significant correlation between bone strength and the mineral properties measured *via* FTIR and lack of correlation with the non-collagenous AGEs.

4. Discussion

In this study, we showed that the accumulation of fluorescent AGEs was not the main contributing factor to bone fragility in long-term type-2 diabetic (*fa/fa*) rats and suggest that diabetic bone disease occurs through a multifactorial mechanism, possibly arising from an altered bone turnover process. For this, we used a factor-by-factor approach to investigate the (i) geometrical, (ii) structural, (iii) material and (iv) compositional properties of tissue in the presence of diabetes through a ZDF (*fa/fa*) rat model at different stages of the diseases: at 12- (Early-stage diabetes), 26- (Established diabetes) and 46-weeks (Long-term diabetes) old. To the authors' knowledge, this is the first ZDF (*fa/fa*) longitudinal animal study investigating long-term diabetic bone fragility in rats up to 46-weeks of age. This study demonstrated that longitudinal diabetic bone growth was impaired as early as 12-weeks of age and by 46-weeks, bone size was significantly lower than healthy controls. The geometrical deficits were reflected in the structural properties. In particular, long-term (46-weeks) diabetic rats were structurally compromised with a lower bending rigidity and energy-to-failure than controls. Importantly, we found that, independently of the structural deficits, the material tissue-level properties of type-2 diabetic bone were impaired. Long-term diabetic (*fa/fa*) rats had a significant reduction in yield and ultimate stress in comparison to their age-matched controls. Interestingly, post-yield displacement (structural property) and toughness (material property) was negatively affected by disease duration within the diabetic strain. Compositional differences were also found in long-term diabetic (*fa/fa*) subjects, with higher AGE accumulation in bone and skin samples in type-2 diabetic subjects, as mineral alterations observed through FTIR analysis, with a reduction in carbonate:phosphate (C:P) ratio and an increase in acid phosphate (AP) content. Importantly, we found that AGEs measured from both bone and skin sections had no correlation with tissue-level strength. We also found that other distinct alterations such as C:P ratio and AP content were associated with tissue level strength.

Individuals with T2D have a greater risk of fracture than non-diabetic [3] and it is understood that the duration of the disease plays a role in fracture risk [4,5,35,36]. The effects of T2D on bone strength has been explored through various *in-vitro* [17–21] and *in-vivo* studies [23,40]. However, T2D is a complex disease that *in-vitro* studies are not yet able to adequately mimic and there is limited availability of human tissue for testing and a large variability in intensity and duration of the disease, which implies a lack of quantitative tissue-level data on type-2 diabetic bone for the same stage of the disease. Our longitudinal study investigated bone fragility in ZDF (*fa/fa*) and control rats at 12- (Early-stage diabetes), 26- (Established diabetes) and 46-weeks (Long-term diabetes). To our knowledge, this is the first type-2 diabetic longitudinal

animal study aging ZDF (*fa/fa*) rats up to 46-weeks of age. Previous to our study, Saito *et al* explored bone fragility in diabetic WBN/Kob rats aged up to 72 weeks (18 months), however, this strain of diabetic rat becomes spontaneously diabetic between 48 and 52 weeks of age, meaning these rats were only diabetic for approximately 24–28 weeks [67]. However, in our study, these ZDF (*fa/fa*) rats become spontaneously diabetic between 9 and 11 weeks old, meaning these rats were overtly diabetic for approximately 35–37 weeks. Our results have shown that, ZDF (*fa/fa*) rats experienced a reduction in bone strength in comparison to controls and that disease duration played a role in this. Moreover, post-yield displacement results demonstrated that long-term diabetic rats had reduced ductility in comparison to younger diabetic rats. This highlights that, as the diseased progressed, long-term diabetic bones fractured in a more brittle manner than short-term diabetic bones. We did not find a difference in post-yield displacement between strains at 46-weeks. However, we did find that in comparison to controls, diabetic rats had a reduced ability to resist deformation due to deficits in bending rigidity, a reduced ability to resist fracture due to reduced energy-to-failure and could not withstand as high a load due to lower ultimate moments. This is similar to what has been previously reported in work by Prisby *et al* where ZDF (fa/fa) (T2D) rats showed no changes in post-yield displacment but did see differences in the energy-to-failure [35]. Similarly, work by Creecy *et al,* which used ZDSD rats, found no difference is post-yield displacement between strains at any age but did find differences in Energy-to-failure of radius bone at all ages [36]. Nevertheless, the negative effects on the structural properties of these diabetic rats can, for the most part, be attributed to the geometrical deficits of these ZDF (*fa/fa*) diabetic rats. This is further shown by the IGF-I levels of the diabetic (*fa/fa*) rats which indicates the dysfunction of their bone growth. The short bone phenotype has also been reported in other studies that have used the ZDF (*fa/fa*) strain as their type-2 diabetic subjects, where the smaller sized bones have been proposed as a phenotype of the ZDF (*fa/fa*) strain [33,35]. Despite the variety of animal studies that have investigated the fracture mechanics of type-2 diabetic bone [33,41,68,69], few studies have explored tissue material properties and often bones with a less favourable geometry for bending or measuring tissue properties are examined, according to their aspect ratio (span length: bone width). Where Jepsen *et al* states that using a slender bone such as the radius, can increase the aspect ratio leading to a more accurate estimation of the elastic modulus [48]. Similarly, the ulna is also considered a slender bone. Importantly, this study highlighted that both structural- and tissue-level properties of ZDF (*fa/fa*) rats were impaired. Indeed, rats with long-term (46-weeks) T2D showed a reduction in tissue yield and ultimate stress. Although the elastic modulus of diabetic (*fa/fa*) bone tended towards being lower than controls (*fa/+*), this was not significant due to greater variability which is expected in *in vivo* studies. This is similar to a previous study, which have found no differences in modulus of elasticity but did find reductions in bone strength between T2D rats and controls [35]. This may also be due to the significant difference in aspect ratio between diabetic and controls at 46-weeks due to significant difference in bone length growth. However, some studies did not go as far as to measure the material-properties following a structural analysis [41,67,69]. Several other studies have found some material level differences, whereby yield and/or ultimate strength of diabetic ulnar [34] or vertebral [33,70] bone was found to be lower than their healthy counterparts. Our results reveal that as the disease progressed the tissue itself, regardless of bone geometry, became impaired with reductions in bone strength observed.

A novel contribution of this study is that we measured tissue composition through FTIR and fAGE analysis at 12-, 26-and 46-weeks. The extent to which bone quality may be affected during T2D is not fully understood and there is a lack of understanding of the sub-tissue alterations that take place during T2D. Our results demonstrated that in long-term (46-weeks) ZDF (*fa/fa*) rats, skin AGE concentration was higher than controls, but there was no difference in cortical bone AGE levels between strains at any age. Studies have suggested that elevated levels of non-enzymatic glycated cross-links leads to a deterioration in tissue properties [23,67]. However, to date, there is still no causal relationship between AGE accumulation and T2D, since previous work measuring bulk fAGEs have shown that diabetic subjects have higher [34,41,72,73] or unchanged levels [23,36,40,69] in comparison to controls. Indeed, increased blood glucose levels can interfere with bone homeostasis [74–76]. Recent work by Entz *et al* found that when the extracellular matrix was produced by human bone marrow adipocytes osteoblastogenesis was not affected, but disruption to the mineralization phase of osteoblasts was observed [77]. Furthermore, when a high glucose environment was introduced they found differential alterations in mineralization quality [77]. Interestingly, through FTIR analysis we demonstrated that some mineral constituents at the sub-tissue level, such as carbonate:phosphate (C:P) ratio and acid phosphate (AP) content, were altered as a result of some possible metabolic impairment due to the hyperglycaemic environment. Both carbonate (CO_3^{2-}) and acid phosphate (HPO_4^{2-}) are the main ions that substitute into the apatite mineral lattice during the modelling and remodeling of bone. However, it is important to note that rodent cortical bone does not remodel in the same way human bone would remodel due to their lack of a well-developed Haversian system like humans. Instead, it is thought that rat bones continue to grow in their outer cortex and the marrow side continues to be resorbed throughout life. Conversely, there has been some evidence to suggest that rodent bone may also be remodelled on intracortical surfaces after maturation, since it is highly vascularised with transcortical vessels containing both osteoclast and osteoblast progenitors [78–81], similar to how Haversian systems continue to be remodelled, with intracortical blood vessels in human bone during adulthood [82,83]. We observed that both properties were associated with tissue strength across both groups. Long-term diabetic (*fa/fa*) rats had a 10 % ($p < 0.05$) reduction in C:P ratio in comparison to controls. Interestingly, previous studies have found that a reduction in C:P ratio has been linked to an increased risk of fracture [51] as well as an accumulation of bone micro-damage [84]. In addition, a reduced C:P ratio has also been seen in patients presenting with low or high bone turnover [85,86] and in fact may convey a lack in type-B carbonate substitutions and thus resulting in a lack of bone maturation during the mineralization process [87]. We also found that long-term diabetic (*fa/fa*) rat bone had 10 % (95 % CI: 1 %, 19 %, $p < 0.05$) more AP content than controls. Acid phosphate content is usually present at high concentrations in young, immature bone, which explains the elevated levels of AP content in 12-week old diabetic (*fa/fa*) rats while the young bones are still modelling [54,88]. However, higher levels of AP content in 12-week diabetic (*fa/fa*) rats than controls may indicate that bone modelling was altered in early stages of bone growth and development. By 46-weeks it is possible that a high AP content may be indicating that secondary mineralization is not proceeding correctly suggesting bone turnover is also affected [59,89]. Considering that a low C:P ratio could indicate a lack of bone maturation, the latter argument is supported in our data from the 46-week old diabetic (*fa/fa*) rats with a long-term exposure to a high glucose environment. This may also suggest further secondary health complications that might be affecting the bone turnover process such as, chronic renal dysregulation, kidney disease, reduced bone vascularisation or metabolic acidosis, which should be explored further in future studies. Therefore, this study indicates that AGE accumulation is not a main contributing factor to bone fragility in these ZDF (*fa/fa*) rats. Instead, results from our FTIR analysis indicates that the impaired mechanical integrity of the bone tissue is a multifactorial mechanism influenced by an altered bone turnover process that reduces bone quality and impairs biomechanical properties as the disease progresses. The basic building block of the ordered material, bone, majorly consists of mineralized collagen fibrils, which are found at the nanoscale. These mineralized organic collagen fibrils are composed of hydroxyapatite mineral crystals and non-collagenous proteins, representing the reinforcement and compliant matrix phase, respectively [90–92]. These hydroxyapatite mineral crystals and collagen fibrils give

bone its stiffness, strength and ductility, respectively, during loading. Our correlation results reveal that the mineral properties were altered, with a reduction in C:P ratio and increase in AP content in long-term diabetic (*fa/fa*) rats which may play a role in reducing the ultimate strength and yield strength of the bone tissue, respectively. Hence, we can hypothesize that the weakness of the long-term diabetic bone in these ZDF (*fa/fa*) rats is related to the mineralization process, whereby the apatite lattice structure is distorted or not maturing into stable hydroxyapatite. It is worth noting that the disruption of the mineral properties occurs in long-term diabetic (*fa/fa*) rats after a prolonged duration with the disease where the rats have not been administered any insulin, medications or a diet or lifestyle change; it is unlikely for patients with long-term T2D to never have some form of intervention throughout the duration of their disease.

There are several limitations and future recommendations that should be noted. The ZDF (*fa/fa*) rat model has a leptin receptor deficiency due to an amino acid substitution, which has been observed in children that possess congenital leptin receptor deficiencies [30,93]. As a result, these rats experience an insatiable appetite, causing them to become overtly diabetic and obese at approximately 9-weeks of age [93]. These rats reach skeletal maturity when they are around 12-weeks old, at which point they also develop a frank-like diabetic condition [33]. In our study, we started the high fat diet at approximately 10-weeks of age, before these rats reached skeletal maturity. It is thought that loss of function of their leptin-receptors may influence the bone size. However, it is also likely that the early onset of T2D before they reached puberty may have influenced their longitudinal stunt in growth. Although there is currently no single animal model that represents all features of T2D in humans; with a rise in the incidence of T2D in children and adolescents in the United States, Australia, China, Canada and United Kingdom [94–99] and a great lack of data that explores the ramifications of long-term diabetes in patients with youth-onset type-2 diabetes [100], it is possible that this ZDF (*fa/fa)* strain may be a suitable animal model to mimic the progression of T2D when developed during childhood or adolescence. Especially since we know the exact time-point of the onset of diabetes in this strain. Additionally, this model is also representative of the small, but still existent, population of humans that develop T2D as a result of a leptin or leptin receptor deficiency [101].

In addition, at approximately 44-weeks of age diabetic (*fa/fa*) rats began to lose body mass, due to a loss of appetite and/or a worsening of their illness. This loss in weight has been observed in both ZDF (*fa/fa*) and ZDSD rats [33,35,36] with disease progression and may be a limitation of these rat strains in modelling long-term diabetes without some form of intervention (*e.g.* insulin or medications). However, a similar study has not found body mass to be a significant explanatory variable for bending strength [36] although it may present as a possible confounding effect. In our study, diabetic (*fa/fa*) rats were switched from a high fat diet to a normal diet to help to mitigate their illness at approximately 42-weeks. Hence, at 46-weeks diabetic rats have lower blood-glucose levels than diabetic (*fa/fa*) rats at 26-weeks. This may also have been due to their loss of appetite. Nonetheless, diabetic rats at 46-weeks still have higher blood glucose levels in comparison to the age-matched controls. Interestingly, previous research has found accumulating evidence to suggest that a disruption of insulin and the growth hormone IGF-I homeostasis in diabetic subjects may be responsible for skeletal deficits [102] and increased vertebral fracture risk [103,104]. In our study, at 12- and 26-weeks controls demonstrated a trend towards and significantly higher serum IGF-I levels than age-matched diabetic (*fa/fa*) rats, respectively. As growth and development slowed with age, IGF-I levels decreased for 46-weeks old controls. However, the levels of IGF-I remained low for diabetic (*fa/fa*) rats, leading to a possible explanation for the stunt in growth for these ZDF (*fa/fa*) rats. Studies have also shown that high glucose concentrations or the presence of AGEs impair the stimulatory actions of IGF-I on osteoblasts [105,106]. Previous research investigating childhood obesity and T2D, found that during puberty IGF-I levels rose and fell in a pattern similar to the rise and fall of insulin resistance, suggesting that the growth hormone IGF-I axis contributes to the insulin resistance of puberty [107]. Thus, it may be useful for future studies to explore serum IGF-I levels in patients with T2D, to help understand bone growth, development and fragility in this disease. Additionally, our results do not reflect the clear increase in bulk fAGEs with disease progression, as was seen in previous work on human bone [108,109]. Nor do we see a similar trend of results from surrogate measurements of AGE levels taken from the skin when compared to bone. This may be by explained by the fact that the fAGE technique is a bulk measurement for AGEs, including pentosidine, crossline and vesperlysines A, B & C to name a few. However, the extent of how quantifiable each AGE is through this fluorescent assay is unknown and some AGEs are better correlated with bone than others, such as the non-fluorescent AGE, carboxymethyl-lysine (CML) [110]. Future work should explore different techniques such as high-performance liquid chromatography (HPLC) and mass spectrometry to quantify individual AGEs, in particular CML and pentosidine, rather than a bulk fAGE approach. A final limitation to this study, is that when preparing our bone powder samples for ATR-FTIR the samples were left to dry overnight in air at 37 °C. It is possible that exposing these samples to air for a long period of time could potentially allow the collagen to become oxidised and denatured. In future it might be better to reduce drying time or temperature when trying to remove water from the samples. Nevertheless, all samples underwent the same preparation and therefore are comparable in this study. Additionally, it may be important to note that if samples are to be used for FTIR analysis and are stored in PBS following dissection, this may affect the FTIR spectra. However, in this study our samples were not immersed in PBS, they were surrounded by gauze with PBS and immediately frozen before mechanical testing, Since the samples were immediately frozen it is unlikely the PBS would have greatly permeated into the bone tissue.

5. Conclusions

This study found that long-term ZDF (*fa/fa*) rats had a reduced tissue-level yield and ultimate strength in comparison to controls, regardless of the geometrical deficits of this rat strain. The reduced tissue material strength coincided with the mineral properties C:P ratio and AP content but was not associated with AGE content. This indicates that bone fragility in these ZDF (*fa/fa*) rats occurs through a multifactorial mechanism influenced initially by impaired bone growth and development and proceeding to an altered bone turnover process that reduces bone quality and impairs biomechanical properties with a long-term duration of the disease. However, further work is required to uncover these contributing factors.

CRediT authorship contribution statement

Genna E. Monahan: Conceptualization, Methodology, Formal analysis, Investigation, Visualization, Funding acquisition, Writing – original draft, Writing – review & editing. **Jessica Schiavi-Tritz:** Conceptualization, Methodology, Supervision, Project administration, Writing – review & editing. **Marissa Britton:** Conceptualization, Methodology. **Ted J. Vaughan:** Conceptualization, Methodology, Funding acquisition, Supervision, Project administration, Writing – review & editing.

Data availability

Data will be made available on request.

Acknowledgements

This research received funding from the European Research Council (ERC-2018-StG Grant 804108). The authors acknowledge the facilities

and the scientific and technical assistance of (1) David Connolly, (2) The Experimental Animal User and Breeding Establishment, and (3) Éadaoin Timmins at the Centre for Microscopy & Imaging, all at the University of Ireland Galway.

Appendix A. Supplementary data

Supplementary data to this article can be found online at https://doi.org/10.1016/j.bone.2023.116672.

References

[1] R.J. Valderrábano, M.I. Linares, Diabetes mellitus and bone health: epidemiology, etiology and implications for fracture risk stratification, Clin. Diabetes Endocrinol. 4 (1) (2018) 9, https://doi.org/10.1186/s40842-018-0060-9.

[2] L. Karim, M.L. Bouxsein, Effect of type 2 diabetes-related non-enzymatic glycation on bone biomechanical properties, Bone 82 (2016) 21–27, https://doi.org/10.1016/j.bone.2015.07.028.

[3] M. Janghorbani, D. Feskanich, W.C. Willett, F. Hu, Prospective study of diabetes and risk of hip fracture, Diabetes Care 29 (7) (2006) 1573–1578, https://doi.org/10.2337/dc06-0440.

[4] J.W. Folk, A.J. Starr, J.S. Early, Early wound complications of operative treatment of calcaneus fractures: analysis of 190 fractures, Available: J. Orthop. Trauma 13 (5) (1999) https://journals.lww.com/jorthotrauma/Fulltext/1999/06000/Early_Wound_Complications_of_Operative_Treatment.8.aspx.

[5] M. Retzepi, N. Donos, The effect of diabetes mellitus on osseous healing, Clin. Oral Implants Res. 21 (7) (2010) 673–681, https://doi.org/10.1111/j.1600-0501.2010.01923.x.

[6] A.M. Parfitt, C.H.E. Mathews, A.R. Villanueva, M. Kleerekoper, B. Frame, D. S. Rao, Relationships between surface, volume, and thickness of iliac trabecular bone in aging and in osteoporosis. Implications for the microanatomic and cellular mechanisms of bone loss, J. Clin. Invest. 72 (4) (1983) 1396–1409, https://doi.org/10.1172/JCI111096.

[7] P. Vestergaard, Discrepancies in bone mineral density and fracture risk in patients with type 1 and type 2 diabetes—a meta-analysis, Osteoporos. Int. 18 (4) (2007) 427–444, https://doi.org/10.1007/s00198-006-0253-4.

[8] M.R. Rubin, J.M. Patsch, Assessment of bone turnover and bone quality in type 2 diabetic bone disease: current concepts and future directions, Bone Res. 4 (1) (2016) 16001, https://doi.org/10.1038/boneres.2016.1.

[9] M. Saito, K. Marumo, Bone quality in diabetes, Front. Endocrinol. (Lausanne) 4 (2013) 1–9, https://doi.org/10.3389/fendo.2013.00072.

[10] R. Dhaliwal, D. Cibula, C. Ghosh, R.S. Weinstock, A.M. Moses, Bone quality assessment in type 2 diabetes mellitus, Osteoporos. Int. 25 (7) (2014) 1969–1973, https://doi.org/10.1007/s00198-014-2704-7.

[11] J.R. Furst, et al., Advanced glycation endproducts and bone material strength in type 2 diabetes, J. Clin. Endocrinol. Metab. 101 (6) (2016) 2502–2510, https://doi.org/10.1210/jc.2016-1437.

[12] A. Goldin, J.A. Beckman, A.M. Schmidt, M.A. Creager, Advanced glycation end products, Circulation 114 (6) (2006) 597–605, https://doi.org/10.1161/CIRCULATIONAHA.106.621854.

[13] M. Yamamoto, T. Sugimoto, Advanced glycation end products, diabetes, and bone strength, Curr. Osteoporos. Rep. 14 (6) (2016) 320–326, https://doi.org/10.1007/s11914-016-0332-1.

[15] T.L. Willett, P. Voziyan, J.S. Nyman, Causative or associative: a critical review of the role of advanced glycation end-products in bone fragility, Bone 163 (March) (2022), 116485, https://doi.org/10.1016/j.bone.2022.116485.

[16] M. Saito, K. Marumo, Collagen cross-links as a determinant of bone quality: a possible explanation for bone fragility in aging, osteoporosis, and diabetes mellitus, Osteoporos. Int. 21 (2) (2010) 195–214, https://doi.org/10.1007/s00198-009-1066-z.

[17] D. Vashishth, G. Gibson, J. Khoury, M. Schaffler, J. Kimura, D. Fyhrie, Influence of nonenzymatic glycation on biomechanical properties of cortical bone, Bone 28 (2) (2001) 195–201, https://doi.org/10.1016/S8756-3282(00)00434-8.

[18] S. Viguet-Carrin, D. Farlay, Y. Bala, F. Munoz, M.L. Bouxsein, P.D. Delmas, An in vitro model to test the contribution of advanced glycation end products to bone biomechanical properties, Bone 42 (1) (2008) 139–149, https://doi.org/10.1016/j.bone.2007.08.046.

[19] J. Catanese, R. Bank, J. TeKoeppele, T. Keaveny, in: Increased Cross-linking by Non-enzymatic Glycation Reduces the Ductility of Bone and Bone Collagen 42, ASME-PUBLICATIONS-BED, 1999, pp. 267–268.

[20] E.A. Zimmermann, et al., Age-related changes in the plasticity and toughness of human cortical bone at multiple length scales, Proc. Natl. Acad. Sci. 108 (35) (2011) 14416–14421, https://doi.org/10.1073/pnas.1107966108.

[21] A.A. Poundarik, et al., A direct role of collagen glycation in bone fracture, J. Mech. Behav. Biomed. Mater. 52 (2015) 120–130, https://doi.org/10.1016/j.jmbbm.2015.08.012.

[22] L. Karim, D. Vashishth, Heterogeneous glycation of cancellous bone and its association with bone quality and fragility, PLoS One 7 (4) (2012), e35047, https://doi.org/10.1371/journal.pone.0035047.

[23] L. Karim, et al., Bone microarchitecture, biomechanical properties, and advanced glycation end-products in the proximal femur of adults with type 2 diabetes, Bone 114 (February) (2018) 32–39, https://doi.org/10.1016/j.bone.2018.05.030.

[24] R.G. Peterson, W.N. Shaw, M. Neel, L.A. Little, J. Eichberg, Zucker diabetic fatty rat as a model for non-insulin-dependent diabetes mellitus, ILAR J. 32 (3) (1990) 16–19, https://doi.org/10.1093/ilar.32.3.16.

[25] N. Yokoi, et al., A novel rat model of type 2 diabetes: the Zucker fatty diabetes mellitus ZFDM rat, J. Diabetes Res. 2013 (2013) 1–9, https://doi.org/10.1155/2013/103731.

[26] H. Chen, et al., Evidence that the diabetes gene encodes the leptin receptor: identification of a mutation in the leptin receptor gene in db/db mice, Cell 84 (3) (1996) 491–495, https://doi.org/10.1016/S0092-8674(00)81294-5.

[27] Y. Lee, H. Hirose, M. Ohneda, J.H. Johnson, J.D. McGarry, R.H. Unger, Beta-cell lipotoxicity in the pathogenesis of non-insulin-dependent diabetes mellitus of obese rats: impairment in adipocyte-beta-cell relationships, Proc. Natl. Acad. Sci. 91 (23) (1994) 10878–10882, https://doi.org/10.1073/pnas.91.23.10878.

[28] C.M. Steppan, D.T. Crawford, K.L. Chidsey-Frink, H. Ke, A.G. Swick, Leptin is a potent stimulator of bone growth in ob/ob mice, Regul. Pept. 92 (1–3) (2000) 73–78, https://doi.org/10.1016/S0167-0115(00)00152-X.

[29] G.J. Etgen, B.A. Oldham, Profiling of Zucker diabetic fatty rats in their progression to the overt diabetic state, Metabolism 49 (5) (2000) 684–688, https://doi.org/10.1016/S0026-0495(00)80049-9.

[30] I.S. Farooqi, et al., Clinical and molecular genetic spectrum of congenital deficiency of the leptin receptor, N. Engl. J. Med. 356 (3) (2007) 237–247, https://doi.org/10.1056/NEJMoa063988.

[31] L.I. Hansson, K. Menander-Sellman, A. Stenström, K.G. Thorngren, Rate of normal longitudinal bone growth in the rat, Calcif. Tissue Res. 10 (1) (1972) 238–251, https://doi.org/10.1007/BF02012553.

[32] P.C. Hughes, J.M. Tanner, The assessment of skeletal maturity in the growing rat, Available: J. Anat. 106 (Pt 2) (1970) 371–402 http://www.ncbi.nlm.nih.gov/pubmed/4315144%0Ahttp://www.pubmedcentral.nih.gov/articlerender.fcgi?artid=PMC1233709.

[33] S. Reinwald, R.G. Peterson, M.R. Allen, D.B. Burr, Skeletal changes associated with the onset of type 2 diabetes in the ZDF and ZDSD rodent models, Am. J. Physiol. Metab. 296 (4) (2009) E765–E774, https://doi.org/10.1152/ajpendo.90937.2008.

[34] C. Acevedo, et al., Contributions of material properties and structure to increased bone fragility for a given bone mass in the UCD-T2DM rat model of type 2 diabetes, J. Bone Miner. Res. 33 (6) (2018) 1066–1075, https://doi.org/10.1002/jbmr.3393.

[35] R.D. Prisby, J.M. Swift, S.A. Bloomfield, H.A. Hogan, M.D. Delp, Altered bone mass, geometry and mechanical properties during the development and progression of type 2 diabetes in the Zucker diabetic fatty rat, J. Endocrinol. 199 (3) (2008) 379–388, https://doi.org/10.1677/JOE-08-0046.

[36] A. Creecy, et al., Changes in the fracture resistance of bone with the progression of type 2 diabetes in the ZDSD rat, Calcif. Tissue Int. 99 (3) (2016) 289–301, https://doi.org/10.1007/s00223-016-0149-z.

[37] H.B. Hunt, et al., Altered tissue composition, microarchitecture, and mechanical performance in cancellous bone from men with type 2 diabetes mellitus, J. Bone Miner. Res. 34 (7) (2019) 1191–1206, https://doi.org/10.1002/jbmr.3711.

[38] H.B. Hunt, et al., Bone tissue composition in postmenopausal women varies with glycemic control from Normal glucose tolerance to type 2 diabetes mellitus, J. Bone Miner. Res. 36 (2) (2021) 334–346, https://doi.org/10.1002/jbmr.4186.

[39] H.B. Hunt, J.C. Pearl, D.R. Diaz, K.B. King, E. Donnelly, Bone tissue collagen maturity and mineral content increase with sustained hyperglycemia in the KK-Ay murine model of type 2 diabetes, J. Bone Miner. Res. 33 (5) (2018) 921–929, https://doi.org/10.1002/jbmr.3365.

[40] E.M. Wölfel, et al., Individuals with type 2 diabetes mellitus show dimorphic and heterogeneous patterns of loss in femoral bone quality, Bone 140 (March) (2020), 115556, https://doi.org/10.1016/j.bone.2020.115556.

[41] P. Sihota, et al., Development of HFD-fed /Low-DoseSTZ-treated female Sprague-dawley rat model to investigate diabetic bone fragility at different organization levels, JBMR Plus 4 (10) (2020) 1–12, https://doi.org/10.1002/jbm4.10379.

[42] F.N. Schmidt, et al., Assessment of collagen quality associated with non-enzymatic cross-links in human bone using Fourier-transform infrared imaging, Bone 97 (2017) 243–251, https://doi.org/10.1016/j.bone.2017.01.015.

[43] M. Janghorbani, R.M. Van Dam, W.C. Willett, F.B. Hu, Systematic review of type 1 and type 2 diabetes mellitus and risk of fracture, Am. J. Epidemiol. 166 (5) (2007) 495–505, https://doi.org/10.1093/aje/kwm106.

[44] W.P. Koh, R. Wang, L.W. Ang, D. Heng, J.M. Yuan, M.C. Yu, Diabetes and risk of hip fracture in the Singapore Chinese health study, Diabetes Care 33 (8) (2010) 1766–1770, https://doi.org/10.2337/dc10-0067.

[45] T. Rezaee, M.L. Bouxsein, L. Karim, Increasing fluoride content deteriorates rat bone mechanical properties, Bone 136 (2020), 115369, https://doi.org/10.1016/j.bone.2020.115369.

[46] M.L. Bouxsein, S.K. Boyd, B.A. Christiansen, R.E. Guldberg, K.J. Jepsen, R. Müller, Guidelines for assessment of bone microstructure in rodents using micro-computed tomography, J. Bone Miner. Res. 25 (7) (2010) 1468–1486, https://doi.org/10.1002/jbmr.141.

[47] J.N. Farr, M.T. Drake, S. Amin, L.J. Melton, L.K. McCready, S. Khosla, In vivo assessment of bone quality in postmenopausal women with type 2 diabetes, J. Bone Miner. Res. 29 (4) (2014) 787–795, https://doi.org/10.1002/jbmr.2106.

[48] K.J. Jepsen, M.J. Silva, D. Vashishth, X.E. Guo, M.C. van der Meulen, Establishing biomechanical mechanisms in mouse models: practical guidelines for systematically evaluating phenotypic changes in the diaphyses of long bones, J. Bone Miner. Res. 30 (6) (2015) 951–966, https://doi.org/10.1002/jbmr.2539.

[49] A.L. Boskey, L. Imbert, Bone quality changes associated with aging and disease: a review, Ann. N. Y. Acad. Sci. 1410 (1) (2017) 93–106, https://doi.org/10.1111/nyas.13572.

[50] N. Kourkoumelis, X. Zhang, Z. Lin, J. Wang, Fourier transform infrared spectroscopy of bone tissue: bone quality assessment in preclinical and clinical applications of osteoporosis and fragility fracture, Clin. Rev. Bone Miner. Metab. 17 (1) (2019) 24–39, https://doi.org/10.1007/s12018-018-9255-y.
[51] B.R. McCreadie, et al., Bone tissue compositional differences in women with and without osteoporotic fracture, Bone 39 (6) (2006) 1190–1195, https://doi.org/10.1016/j.bone.2006.06.008.
[52] M. Gardegaront, D. Farlay, O. Peyruchaud, H. Follet, Automation of the peak fitting method in bone FTIR microspectroscopy spectrum analysis: human and mice bone study, J. Spectrosc. (2018) 1–11, https://doi.org/10.1155/2018/4131029. Figure 1.
[53] D. Farlay, G. Panczer, C. Rey, P.D. Delmas, G. Boivin, Mineral maturity and crystallinity index are distinct characteristics of bone mineral, J. Bone Miner. Metab. 28 (4) (2010) 433–445, https://doi.org/10.1007/s00774-009-0146-7.
[54] S.J. Gadaleta, E.P. Paschalis, F. Betts, R. Mendelsohn, A.L. Boskey, Fourier transform infrared spectroscopy of the solution-mediated conversion of amorphous calcium phosphate to hydroxyapatite: new correlations between X-ray diffraction and infrared data, Calcif. Tissue Int. 58 (1) (1996) 9–16, https://doi.org/10.1007/BF02509540.
[55] A.L. Boskey, et al., Examining the relationships between bone tissue composition, compositional heterogeneity, and fragility fracture: a matched case-controlled FTIRI study, J. Bone Miner. Res. 31 (5) (2016) 1070–1081, https://doi.org/10.1002/jbmr.2759.
[56] H. Ou-Yang, E.P. Paschalis, W.E. Mayo, A.L. Boskey, R. Mendelsohn, Infrared microscopic imaging of bone: spatial distribution of CO32−, J. Bone Miner. Res. 16 (5) (2001) 893–900, https://doi.org/10.1359/jbmr.2001.16.5.893.
[57] J.S. Yerramshetty, O. Akkus, The associations between mineral crystallinity and the mechanical properties of human cortical bone, Bone 42 (3) (2008) 476–482, https://doi.org/10.1016/j.bone.2007.12.001.
[58] A. Boskey, R. Mendelsohn, Infrared analysis of bone in health and disease, J. Biomed. Opt. 10 (3) (2005), 031102, https://doi.org/10.1117/1.1922927.
[59] L. Spevak, C.R. Flach, T. Hunter, R. Mendelsohn, A. Boskey, Fourier transform infrared spectroscopic imaging parameters describing acid phosphate substitution in biologic hydroxyapatite, Calcif. Tissue Int. 92 (5) (2013) 418–428, https://doi.org/10.1007/s00223-013-9695-9.
[60] A.L. Boskey, N. Pleshkocamacho, FT-IR imaging of native and tissue-engineered bone and cartilage, Biomaterials 28 (15) (2007) 2465–2478, https://doi.org/10.1016/j.biomaterials.2006.11.043.
[61] E.P. Paschalis, K. Verdelis, S.B. Doty, A.L. Boskey, R. Mendelsohn, M. Yamauchi, Spectroscopic characterization of collagen cross-links in bone, J. Bone Miner. Res. 16 (10) (2001) 1821–1828, https://doi.org/10.1359/jbmr.2001.16.10.1821.
[62] P. Gkogkolou, M. Böhm, Advanced glycation end products, Dermatoendocrinol. 4 (3) (2012) 259–270, https://doi.org/10.4161/derm.22028.
[63] N.Y. Ignat'eva, N.A. Danilov, S.V. Averkiev, M.V. Obrezkova, V.V. Lunin, E. N. Sobol, Determination of hydroxyproline in tissues and the evaluation of the collagen content of the tissues, J. Anal. Chem. 62 (1) (2007) 51–57, https://doi.org/10.1134/S106193480701011X.
[64] W. Kafienah, T.J. Sims, Biochemical methods for the analysis of tissue-engineered cartilage, in: A.P. Hollander, P.V. Hatton (Eds.), Biopolymer Methods in Tissue Engineering, Humana Press, New Jersey, 2004, pp. 217–230.
[65] J. An, S. Leeuwenburgh, J. Wolke, J. Jansen, Mineralization processes in hard tissue: bone, Biominer. Biomater. Fundam. Appl. (2016) 129–146, https://doi.org/10.1016/B978-1-78242-338-6.00005-3.
[66] C. Ma, T. Du, X. Niu, Y. Fan, Biomechanics and mechanobiology of the bone matrix, Bone Res. 10 (1) (2022), https://doi.org/10.1038/s41413-022-00223-y.
[67] M. Saito, K. Fujii, Y. Mori, K. Marumo, Role of collagen enzymatic and glycation induced cross-links as a determinant of bone quality in spontaneously diabetic WBN/Kob rats, Osteoporos. Int. 17 (10) (2006) 1514–1523, https://doi.org/10.1007/s00198-006-0155-5.
[68] C. Hamann, et al., Effects of parathyroid hormone on bone mass, bone strength, and bone regeneration in male rats with type 2 diabetes mellitus, Endocrinology 155 (4) (2014) 1197–1206, https://doi.org/10.1210/en.2013-1960.
[69] M.J. Devlin, et al., Early-onset type 2 diabetes impairs skeletal Acquisition in the Male TALLYHO/JngJ mouse, Endocrinology 155 (10) (2014) 3806–3816, https://doi.org/10.1210/en.2014-1041.
[70] M.A. Gallant, D.M. Brown, J.M. Organ, M.R. Allen, D.B. Burr, Reference-point indentation correlates with bone toughness assessed using whole-bone traditional mechanical testing, Bone 53 (1) (2013) 301–305, https://doi.org/10.1016/j.bone.2012.12.015.
[72] M.J.L. Tice, S. Bailey, G.E. Sroga, E.J. Gallagher, D. Vashishth, Non-obese MKR mouse model of type 2 diabetes reveals skeletal alterations in mineralization and material properties, JBMR Plus 6 (2) (2022) 1–14, https://doi.org/10.1002/jbm4.10583.
[73] J.E. LLabre, G.E. Sroga, M.J.L. Tice, D. Vashishth, Induction and rescue of skeletal fragility in a high-fat diet mouse model of type 2 diabetes: an in vivo and in vitro approach, Bone 156 (December 2021) (2022), https://doi.org/10.1016/j.bone.2021.116302.
[74] N. Ogawa, T. Yamaguchi, S. Yano, M. Yamauchi, M. Yamamoto, T. Sugimoto, The combination of high glucose and advanced glycation end-products (AGEs) inhibits the mineralization of osteoblastic MC3T3-E1 cells through glucose-induced increase in the receptor for AGEs, Horm. Metab. Res. 39 (12) (2007) 871–875, https://doi.org/10.1055/s-2007-991157.
[75] K. Tanaka, T. Yamaguchi, I. Kanazawa, T. Sugimoto, Effects of high glucose and advanced glycation end products on the expressions of sclerostin and RANKL as well as apoptosis in osteocyte-like MLO-Y4-A2 cells, Biochem. Biophys. Res. Commun. 461 (2) (2015) 193–199, https://doi.org/10.1016/j.bbrc.2015.02.091.
[76] A. Picke, G. Campbell, N. Napoli, L.C. Hofbauer, M. Rauner, Update on the impact of type 2 diabetes mellitus on bone metabolism and material properties, Endocr. Connect. 8 (3) (2019) R55–R70, https://doi.org/10.1530/EC-18-0456.
[77] L. Entz, G. Falgayrac, C. Chauveau, G. Pasquier, S. Lucas, The extracellular matrix of human bone marrow adipocytes and glucose concentration differentially alter mineralization quality without impairing osteoblastogenesis, Bone Reports 17 (September) (2022), 101622, https://doi.org/10.1016/j.bonr.2022.101622.
[78] T. Isojima, N.A. Sims, Cortical bone development, maintenance and porosity: genetic alterations in humans and mice influencing chondrocytes, osteoclasts, osteoblasts and osteocytes, Cell. Mol. Life Sci. 78 (15) (2021) 5755–5773, https://doi.org/10.1007/s00018-021-03884-w.
[79] S.H. Root, et al., Perivascular osteoprogenitors are associated with transcortical channels of long bones, Stem Cells 38 (6) (2020) 769–781, https://doi.org/10.1002/stem.3159.
[80] A. Grüneboom, et al., in: Europe PMC Funders Group Europe PMC Funders Author Manuscripts A Network of Trans-cortical Capillaries as Mainstay for Blood Circulation in Long Bones 1, 2019, pp. 236–250, https://doi.org/10.1038/s42255-018-0016-5.A, 2.
[81] E.C. Walker, et al., Cortical bone maturation in mice requires SOCS3 suppression of gp130/STAT3 signalling in osteocytes, elife 9 (2020) 1–27, https://doi.org/10.7554/eLife.56666.
[82] D.H. Enlow, in: A Study of the Post-Natal Growth and Remodeling of Bone 80, 1985, pp. 270–278, 2.
[83] N.A. Sims, T.J. Martin, Osteoclasts provide coupling signals to osteoblast lineage cells through multiple mechanisms, Annu. Rev. Physiol. 82 (2020) 507–529, https://doi.org/10.1146/annurev-physiol-021119-034425.
[84] M.E. Ruppel, D.B. Burr, L.M. Miller, Chemical makeup of microdamaged bone differs from undamaged bone, Bone 39 (2) (2006) 318–324, https://doi.org/10.1016/j.bone.2006.02.052.
[85] H. Isaksson, et al., Infrared spectroscopy indicates altered bone turnover and remodeling activity in renal osteodystrophy, J. Bone Miner. Res. 25 (6) (2010) 1360–1366, https://doi.org/10.1002/jbmr.10.
[86] H.H. Malluche, D.S. Porter, M.-C. Monier-Faugere, H. Mawad, D. Pienkowski, Differences in bone quality in low- and high-turnover renal osteodystrophy, J. Am. Soc. Nephrol. 23 (3) (2012) 525–532, https://doi.org/10.1681/ASN.2010121253.
[87] G. Velraj, S. Karthikeyan, A. Chitra, Mineralization changes substituted type b carbonate of Po43− ion in the bone minerals of an archaeological sample studied using Fourier self deconvolution technique, Indian J. Biochem. Biophys. 57 (3) (2020) 277–282, https://doi.org/10.56042/ijbb.v57i3.36490.
[88] R. Huang, L. Miller, C. Carlson, M. Chance, Characterization of bone mineral composition in the proximal tibia of cynomolgus monkeys: effect of ovariectomy and nandrolone decanoate treatment, Bone 30 (3) (2002) 492–497, https://doi.org/10.1016/S8756-3282(01)00691-3.
[89] Y. Sai, Y. Shiwaku, T. Anada, K. Tsuchiya, T. Takahashi, O. Suzuki, Capacity of octacalcium phosphate to promote osteoblastic differentiation toward osteocytes in vitro, Acta Biomater. 69 (2018) 362–371, https://doi.org/10.1016/j.actbio.2018.01.026.
[90] T. Hofmann, F. Heyroth, H. Meinhard, W. Fränzel, K. Raum, Assessment of composition and anisotropic elastic properties of secondary osteon lamellae, J. Biomech. 39 (12) (2006) 2282–2294, https://doi.org/10.1016/j.jbiomech.2005.07.009.
[91] J.D. Currey, Effects of differences in mineralization on the mechanical properties of bone, Philos. Trans. R. Soc. Lond. Ser. B Biol. Sci. 304 (1121) (1984) 509–518, https://doi.org/10.1098/rstb.1984.0042.
[92] A. Ascenzi, E. Bonucci, Relationship between ultrastructure and 'pin test' in osteons [Online]. Available: Clin. Orthop. Relat. Res. 121 (1976) 275–294 http://europepmc.org/abstract/MED/991513.
[93] R.J. Fajardo, L. Karim, V.I. Calley, M.L. Bouxsein, A review of rodent models of type 2 diabetic skeletal fragility, J. Bone Miner. Res. 29 (5) (2014) 1025–1040, https://doi.org/10.1002/jbmr.2210.
[94] H. Wu, et al., Worldwide estimates of incidence of type 2 diabetes in children and adolescents in 2021, Diabetes Res. Clin. Pract. 185 (January) (2022), 109785, https://doi.org/10.1016/j.diabres.2022.109785.
[95] J. Divers, et al., in: Morbidity and Mortality Weekly Report Trends in Incidence of Type 1 and Type 2 Diabetes Among Youths-Selected Counties and Indian Reservations, United States, 2002-2015 69, 2002, pp. 161–165, no. 6.
[96] A. Haynes, R. Kalic, M. Cooper, J.K. Hewitt, E.A. Davis, Increasing incidence of type 2 diabetes in indigenous and non-indigenous children in Western Australia, 1990e2012, Med. J. Aust. 204 (8) (2016) 2–3, https://doi.org/10.5694/MJA15.00958.
[97] M. Slater, et al., First nations people with diabetes in Ontario: methods for a longitudinal population-based cohort study, C. Open 7 (4) (2019) E680–E688, https://doi.org/10.9778/cmajo.20190096.
[98] J.Y. Ling Tung, et al., Incidence and clinical characteristics of pediatric-onset type 2 diabetes in Hong Kong: the Hong Kong childhood diabetes registry 2008 to 2017, Pediatr. Diabetes 23 (5) (2022) 556–561, https://doi.org/10.1111/pedi.13231.
[99] T.P. Candler, O. Mahmoud, R.M. Lynn, A.A. Majbar, T.G. Barrett, J.P.H. Shield, Continuing rise of type 2 diabetes incidence in children and young people in the UK, Diabet. Med. 35 (6) (2018) 737–744, https://doi.org/10.1111/dme.13609.
[100] Y. Fan, et al., Incidence of long-term diabetes complications and mortality in youth-onset type 2 diabetes: a systematic review, Diabetes Res. Clin. Pract. 191 (June) (2022), 110030, https://doi.org/10.1016/j.diabres.2022.110030.
[101] A.M. DePaoli, Leptin in common obesity and associated disorders of metabolism, J. Endocrinol. 223 (1) (2014) T71–T81, https://doi.org/10.1530/JOE-14-0258.

[102] T.K. Fowlkes, JL, R.C. Bunn, Contributions of the insulin/insulin-like growth factor-1 axis to diabetic osteopathy, J. Diabetes Metab. 29 (10) (2008) 1883–1889, https://doi.org/10.4172/2155-6156.S1-003.Contributions.

[103] T. Sugimoto, K. Nishiyama, F. Kuribayashi, K. Chihara, Serum levels of insulin-like growth factor (IGF) I, IGF-binding protein (IGFBP)-2, and IGFBP-3 in osteoporotic patients with and without spinal fractures, J. Bone Miner. Res. 12 (8) (1997) 1272–1279, https://doi.org/10.1359/jbmr.1997.12.8.1272.

[104] T. Yamaguchi, et al., Serum levels of insulin-like growth factor (IGF); IGF-binding proteins-3, -4, and -5; and their relationships to bone mineral density and the risk of vertebral fractures in postmenopausal women, Calcif. Tissue Int. 78 (1) (2006) 18–24, https://doi.org/10.1007/s00223-005-0163-z.

[105] A.D. McCarthy, S.B. Etcheverry, A.M. Cortizo, Effect of advanced glycation endproducts on the secretion of insulin-like growth factor-I and its binding proteins: role in osteoblast development, Acta Diabetol. 38 (3) (2001) 113–122, https://doi.org/10.1007/s005920170007.

[106] M. Terada, et al., Growth-inhibitory effect of a high glucose concentration on osteoblast-like cells, Bone 22 (1) (1998) 17–23, https://doi.org/10.1016/S8756-3282(97)00220-2.

[107] T.S. Hannon, G. Rao, S.A. Arslanian, Childhood obesity and type 2 diabetes mellitus, Pediatrics 116 (2) (2005) 473–480, https://doi.org/10.1542/peds.2004-2536.

[108] L. Karim, S.Y. Tang, G.E. Sroga, D. Vashishth, Differences in non-enzymatic glycation and collagen cross-links between human cortical and cancellous bone, Osteoporos. Int. 24 (9) (2013) 2441–2447, https://doi.org/10.1007/s00198-013-2319-4.

[109] D.G. Dyer, et al., in: Accumulation of Maillard Reaction Products in Skin Collagen in Diabetes and Aging CH20H 91, 1993, pp. 2463–2469. June.

[110] C.J. Thomas, T.P. Cleland, G.E. Sroga, D. Vashishth, Accumulation of carboxymethyl-lysine (CML) in human cortical bone, Bone 110 (2018) 128–133, https://doi.org/10.1016/j.bone.2018.01.028.